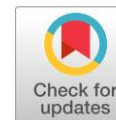


# The oligosuccinimide and modified polysuccinimide as green corrosion and scale inhibitors

Muhamad Jalil Baari \* 

Department of Chemistry, Faculty of Science and Technology, Universitas Sembilanbelas November Kolaka, Kolaka 93517, Indonesia

\* Corresponding Author: [jalilbaari@gmail.com](mailto:jalilbaari@gmail.com)



This paper belongs to a Regular Issue.

## Abstract

Corrosion and scale formation are crucial issues in the petroleum industry. They can inflict metal or other materials breakdown, leading to environmental pollution. Applying scale and corrosion inhibitors is a cost-effective and efficient way of controlling corrosion and scale formation in a fluid system. Much research has been conducted to obtain cheap and safe corrosion or scale inhibitors. Modified polysuccinimides (PSI) are among the organic compounds reported as effective and environmentally friendly corrosion as well as scale inhibitors. The use of various novel green corrosion and scale inhibitors from modified PSI for controlling corrosion reactions or scale formation has not been extensively reviewed. Hence, this review highlights recent studies on preparing PSI/OSI, modifying PSI, and analyzing their performance as corrosion and scale inhibitors. Adsorption study, biodegradation performance, computational quantum study, limitations, and prospects of the inhibitors are also discussed. Therefore, this work provides an overview of novel modified PSI as effective and safe corrosion or scale inhibitors in different media, for various metals, and on a different scale.

## Keywords

oligosuccinimide  
polysuccinimide  
corrosion  
scale  
corrosion inhibitor  
scale inhibitor

Received: 15.02.23

Revised: 12.03.23

Accepted: 12.03.23

Available online: 17.03.23

## Key findings

- Various methods of synthesizing polysuccinimide are outlined.
- Several modified PSI used as corrosion and scale inhibitors in 2015–2022 are reported.
- Adsorption types, energy, isotherm, biodegradation performance, and inhibitor type from modified PSI are listed.
- Computational study results, limitations, and future prospects of modified PSI as corrosion and scale inhibitor are overviewed.

© 2023, the Authors. This article is published in open access under the terms and conditions of the Creative Commons Attribution (CC BY) license (<http://creativecommons.org/licenses/by/4.0/>).

## 1. Introduction

Inorganic scale deposition is a general problem in water cooling and oil wells systems [1–3]. There are several ordinary types of scales, for instance, calcium sulfate ( $\text{CaSO}_4$ ), barium sulfate ( $\text{BaSO}_4$ ), calcium carbonate ( $\text{CaCO}_3$ ), and calcium phosphate ( $\text{Ca}_3(\text{PO}_4)_2$ ). These scales precipitate on several parts of the pipeline surface as well as the water cooling system, generating pipeline blockage and a reduction in the heat exchanger's performance [4]. Thus, scaling increases energy consumption and leads to unscheduled shutdown time, reduction of heat transfer, and some plant accidents [5–7]. The other scale formation

consequences are disruptions in water treatment installation. Besides scales, another common problem is metal corrosion. It corresponds to the degradation of the pipeline due to electrochemical reactions during oil-gas transportation from the oil wells to the processing and storage facilities. In the system of cooling water, corrosion occurs through the utilization of water coolant for heating control during the production process. In addition, the presence of scales generates a more aggressive corrosion process on the pipeline than the main corrosive species, such as inorganic salts, dissolved gas, or microorganisms [8, 9]. Scales cause pitting corrosion that inflicts pipeline leakage and oil spills.

Several techniques have been applied to control corrosion and scale formation. Corrosion reaction on metal can be controlled by using corrosion-resistance material [10, 11], coating/painting [12–14], and corrosion inhibitors [15–17]. Meanwhile, scaling can be solved physically, by the ultrasonic wave and magnetic field, or chemically, by pickling, acidification, and scale inhibitors [18–20]. Corrosion (CI) and scale inhibitors (SI) were reported as cost-effective and efficient techniques for solving those problems. Nowadays, water-soluble and biodegradable polymers and oligomers are attracting the attention of many researchers in the field of corrosion and scale inhibitors [21–23]. Various studies have been conducted to obtain good polymer-based corrosion and scale inhibitors. Besides the effectiveness, the environmental factor must be concerned when choosing polymer as a potential inhibitor. Polysuccinimide (PSI) is an example of a polymer that is usually used as CI and SI. The molecular structure of PSI consists of *N*-heterocyclics with five-member rings. The presence of heteroatoms like nitrogen and oxygen affects the interaction strength between PSI with metal or metal ions through ionic chelation reactions [24, 25]. These heteroatoms lie in carbonyl/amide functional groups in the PSI molecular structure.

PSI is a biodegradable and non-toxic compound, safe for the environment. Lysosomal enzymes, for example, can degrade PSI and its derivatives [26]. Fungi and microorganisms can also degrade them to produce safe compounds [27]. Phosphorus element, which plays a role in the eutrophication process causing water environmental problems, is not present in these compounds [28]. However, PSI is rarely applied in various fields because of its water-insoluble nature. PSI needs to be modified first to change its solubility properties. These modifications can be in the form of an initial synthesis method from the precursors. The reactions of PSI with other substances will open its rings or form a copolymer/composite.

Several review articles discuss polyaspartic acid (PASP) and its derivatives for many applications. However, the exposure of PSI as an initial compound of PASP and the focus of its application as the corrosion and scale inhibitor have not been sufficiently reviewed. Therefore, this review focuses on a discussion of the synthesis method of PSI, modifications of PSI, and its utilization as corrosion and scale inhibitor. Besides that, the oligomer form of polysuccinimide or oligosuccinimide (OSI) is also mentioned. Research results are summarized and reorganized to provide information about the developments of modified PSI as corrosion and scale inhibitors, adsorption study, biodegradation performance, computational quantum study, limitations, and prospects. The reviewed studies were obtained from the articles published in 2015–2022. Most PSI derivations are  $\text{CaCO}_3$ ,  $\text{CaSO}_4$ ,  $\text{BaSO}_4$ , and  $\text{Ca}_3\text{PO}_4$  scale inhibitors. Moreover, the others were used as corrosion inhibitors in various met-

als/alloys and media. Then, there are modified PSI with dual functions applied as corrosion and scale inhibitors.

## 2. Preparation of polysuccinimide

PSI or OSI is mainly synthesized from various starting materials through chemical reactions. Figure 1 displays several ways to synthesize PSI/OSI. Some studies reported reactions between maleic anhydride and ammonium carbonate [29, 30], maleic anhydride and urea [20, 27, 31, 32], maleic anhydride and ammonia [31], maleic anhydride and ammonium hydroxide [33], *L*-aspartic acid and liquid 1-ethyl-3-methylimidazol dihydrogen phosphate [34], and the mixture of maleic anhydride, ethanol, ammonia, *N*-methyl pyrrolidone and sulfolane [35]. Besides that, PSI can also be synthesized through thermal polycondensation of *L*-aspartic acid [36].

Baari et al. [41] reported the presence of more end groups of OSI after condensation reactions between maleic anhydride and ammonium carbonate. The succinimide, amino, and maleimide end groups were based on NMR spectroscopy. The previous study also revealed that synthesis of PSI through microwave-enhanced polycondensation of *L*-Aspartic Acid produces PSI with several end groups and main chains, for instance, maleimide end group, amino end group, succinimide end group, fumaramic end group, alanyl, and fumaramide units in the main chain [37]. This can be called irregular structures of PSI. Hence, precursor types and synthesis methods affect the molecular structures of synthesized PSI.

Sun et al. [31] reported different performances of modified PSI in the form of poly(aspartic acid)-tryptophan grafted copolymer from two synthesis routes [31]. Both copolymer or PASP with maleic anhydride and urea as precursors have better scale inhibition performance than copolymer and PASP from PSI synthesized by maleic anhydride and ammonia. Irregular structures in the PASP and copolymer may determine their chelating capability. However, the production of PSI from maleic anhydride and urea needs additional chemicals like sulfuric acid and phosphoric acid. It will slightly increase chemical waste and cost.

Meanwhile, the utilization of *L*-aspartic acid and liquid 1-ethyl-3-methyl imidazole dihydrogen phosphate to form PSI contains phosphorus elements. This element is quite dangerous for the environment due to the risk of secondary pollution [28, 38]. PSI could be synthesized from a starting material, *L*-aspartic acid, through polycondensation. It is a more straightforward process, but more expensive, because it requires the *L*-aspartic acid provision.

Some PSI or OSI were synthesized through thermal condensation without an organic solvent. Hence, the production process tends to be safe for the environment because it does not generate more chemical waste.

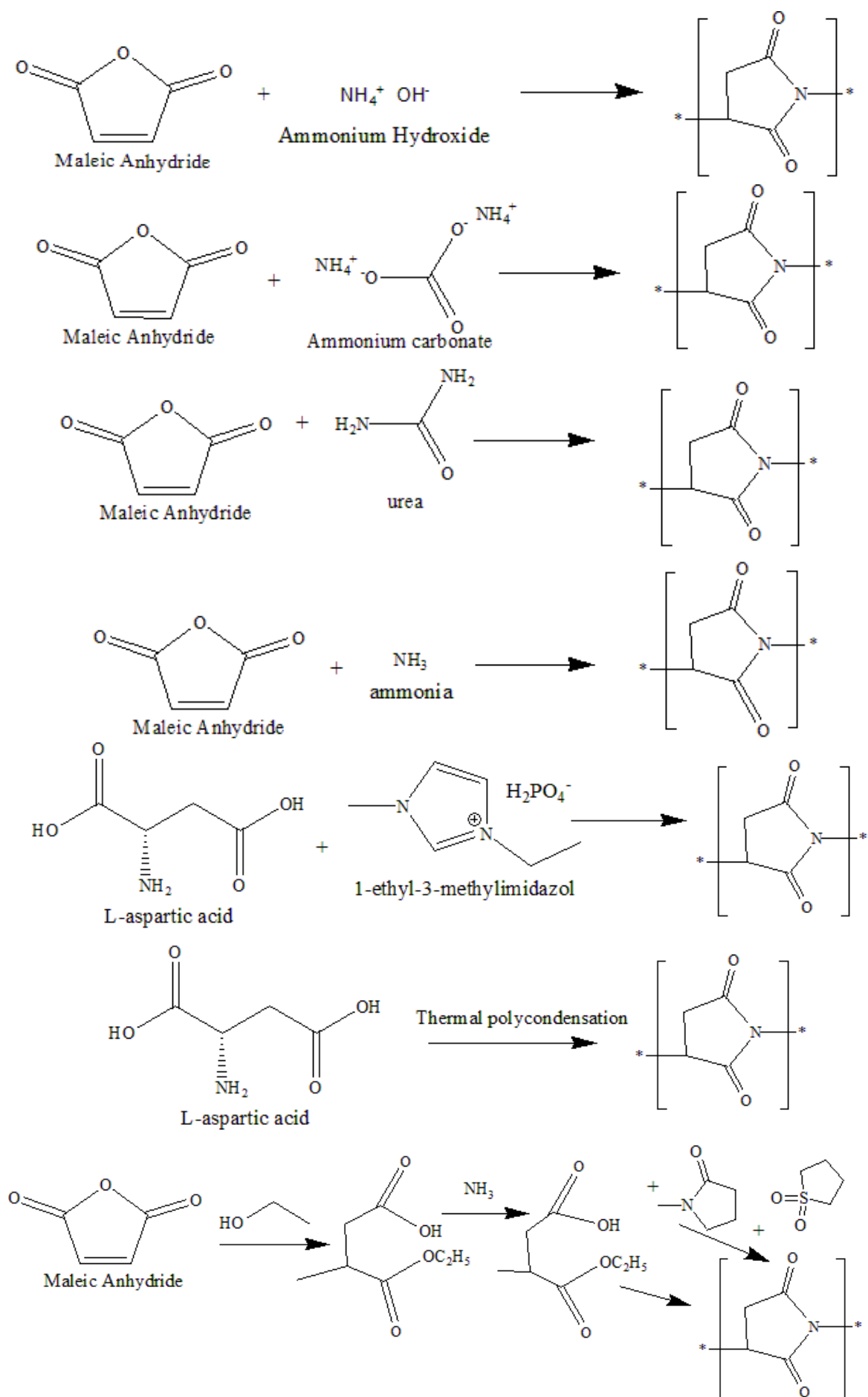


Figure 1 Schemes for synthesizing OSI/PSI. Some of those are reproduced from [29, 32].

### 3. Modification of polysuccinimide

PSI, as the main compound, should usually be converted to polyaspartic acid (PASP) owing to low water solubility, thus limiting its utilization. PASP is a reddish-brown solid compound. It has opening ring structures that are more reactive than PSI. PASP is an intermediate compound to synthesize modified PSI with target properties. The synthesis process occurs through chemical reactions among PASP and other substances under certain conditions [39]. Different procedures have been carried out to directly mix PSI and other substances or form an oligomer form of PSI (oligosuccinimide). Polyaspartic acid/diethylenetriamine graft copolymer, dopamine-modified polyaspartic acid, and cysteamine-modified polyaspartic acid are examples of modified PSI without forming PASP first [3, 32, 40]. Synthesis schemes of various modified PSI are displayed in Figure 2–6. Meanwhile, oligosuccinimide (OSI) has better water solubility than PSI. Hence, it can be directly used as a corrosion and scale inhibitor without modification [29, 41].

Characterizations are conducted to observe structure, crystallinity, thermal stability, etc. OSI and PSI have similar peaks in their  $^1\text{H}$  NMR spectra based on [35, 41] studies. The differences were in solvent peaks, chemical shifts of the peaks, and irregular structure in the primary or end groups. Peaks from residual solvent often appear on  $^1\text{H}$  NMR spectra. OSI used  $\text{D}_2\text{O}$  as a solvent in NMR characterization, while PSI often used  $(\text{CD}_3)_2\text{SO}$ . The discrepancy can also originate from chain length or molecular weight. In addition, FTIR spectra also displayed similar peaks between OSI and PSI [29]. It is obtained from vibrations of identical functional groups. Then, the use of OSI and modified PSI as corrosion and scale inhibitors must be noticed. It is related to these compounds' biodegradation capability and toxicity based on the international regulations.

### 4. Utilizations of oligosuccinimide and modified polysuccinimide as corrosion and scale inhibitors

#### 4.1. Corrosion inhibitor

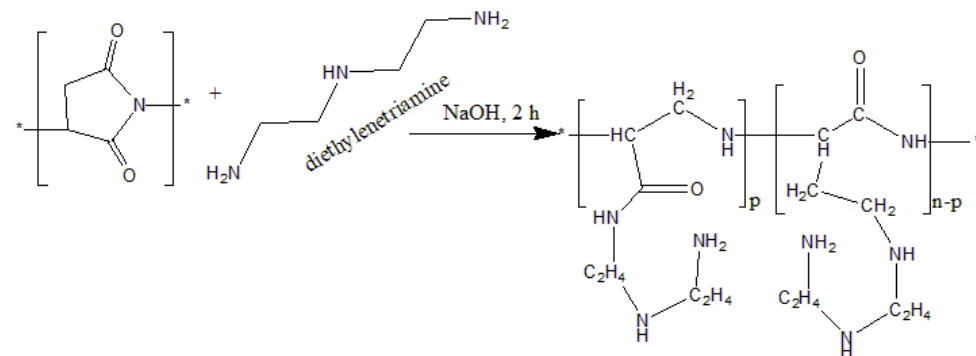
This section discusses the performance of modified PSI as corrosion inhibitors in variegated methods. Several analysis methods were applied: weight loss, potentiodynamic polarization (PDP), and electrochemical impedance spectroscopy (EIS). There are three types of corrosive/electrolyte solutions in the use of modified PSI as corrosion inhibitors, for example, NaCl,  $\text{H}_2\text{SO}_4$ , and artificial seawater solutions. NaCl and artificial seawater solutions were used for conforming to general conditions in petroleum transportation through a pipeline. Then, using an  $\text{H}_2\text{SO}_4$  solution correlates to acidification in the system to overcome scale formation. These types of corrosive so-

lutions may influence the ability of the inhibitor to reduce the corrosion rate.

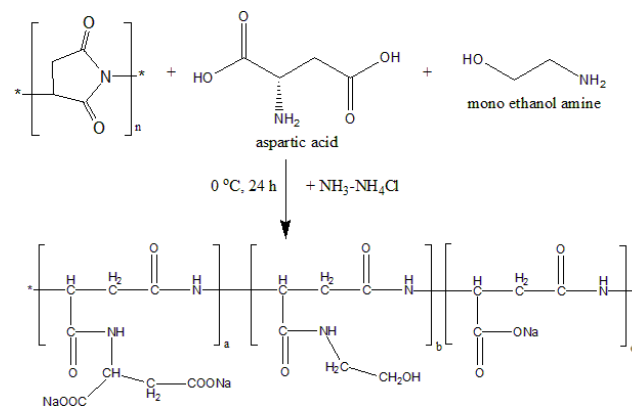
A summary of oligomer form and modified PSI as corrosion inhibitors is listed in Table 1. The corrosion inhibition ability of PASP in each study is also mentioned in comparison. Table 1 shows that advanced modified PSI is a better corrosion inhibitor than PASP. Most of the modified PSI have inhibition efficiencies  $>90\%$ , whereas inhibition efficiency of PASP is below  $90\%$ . Additional heteroatoms, functional groups, and double bonds in modified PSI mitigate electrochemical reactions efficiently on the metal surface as a trigger for the corrosion process [40].

The presence of Zn ions in the modified PSI increases corrosion inhibition efficiency. If modified PSI tends to prevent oxidation reactions on the anodic site, Zn ions can slow electrochemical reactions in the cathodic area [36]. Besides that, Zn ions can also accelerate protective film formation on the metal surface. Therefore, the synergy of Zn ions and modified PSI achieves higher inhibition efficiency. Modified PSI can be fabricated from two types of polymers. Polyaspartic acid/chitosan complex and polyaspartic acid/chitosan graft copolymer are some of the examples [39, 45]. They are formed from PASP and chitosan, which are biodegradable compounds. However, polyaspartic acid/chitosan complex forms a composite that generates a multicomponent system, while polyaspartic acid/chitosan graft copolymer is a single-phase substance. Compared to chitosan and PASP, polyaspartic acid/chitosan complex and polyaspartic acid/chitosan graft copolymer show higher corrosion inhibition efficiency for carbon steel in NaCl solution. The presence of more polar functional groups like hydroxyls, carbonyls, and amines in one copolymer/composite molecule enhances the adsorption of inhibitors on the metal surface. Then, hydrophobic parts of inhibitor molecules are on the outer side to prevent contact between dissolved oxygen, corrosive ions, and water with tested metal [47]. Meanwhile, the composite has a slightly better corrosion inhibition than the copolymer form. It may be related to additional double bonds from glutaraldehyde as cross-linker, whereas the copolymer form is also effective as  $\text{CaCO}_3$  and  $\text{Ca}_3(\text{PO}_4)_2$  scale inhibitor. A significant difference between copolymer and composites forms of chitosan-PASP is in the pH effect. The inhibition efficiency of polyaspartic acid/chitosan composite increases with increasing pH. On the contrary, polyaspartic acid/chitosan graft copolymer is more effective in lower pH.

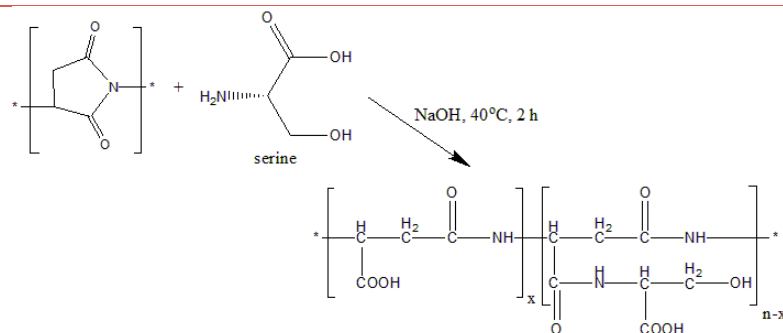
Dopamine-modified polyaspartic acid shows high corrosion inhibition efficiency ( $>90\%$ ) [40]. Besides hydroxyl, carbonyl, and amine groups, this modified PSI also contains aromatic rings in its molecular structure. The presence of these aromatic rings contributes to enhancing the inhibition performance of corrosion inhibitors. Additional electron donors augment the number of inhibitor molecules interacting/bonding with Fe atoms.



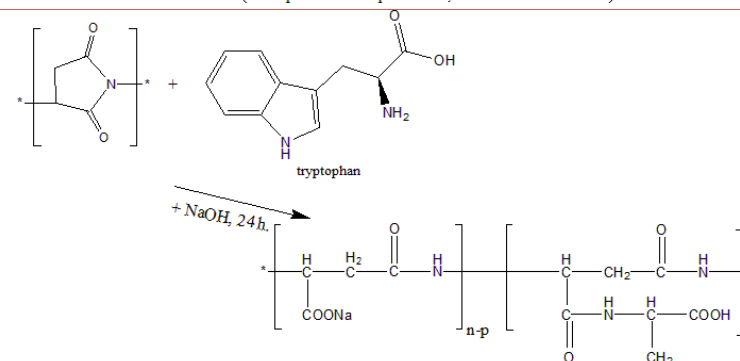
Polyaspartic Acid/Diethylenetriamine Graft Copolymer



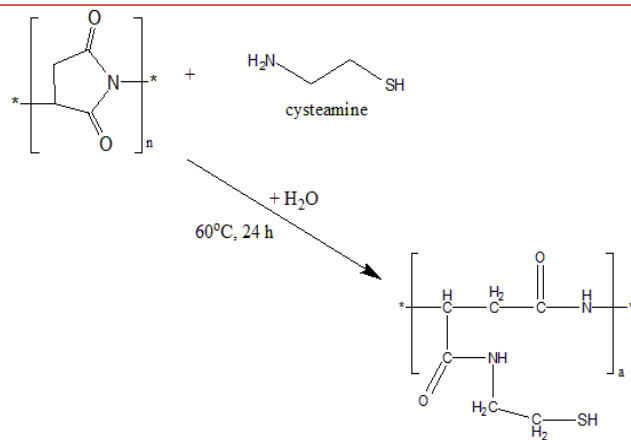
Ring-Opening Graft Modification of Polyaspartic Acid (Polyaspartic acid- aspartic acid, and monoethanolamine)



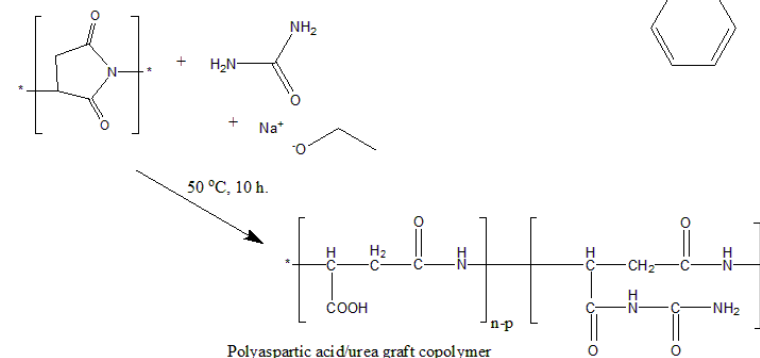
Polyaspartic acid-serine grafted copolymer



Poly(aspartic acid)-tryptophan grafted copolymer

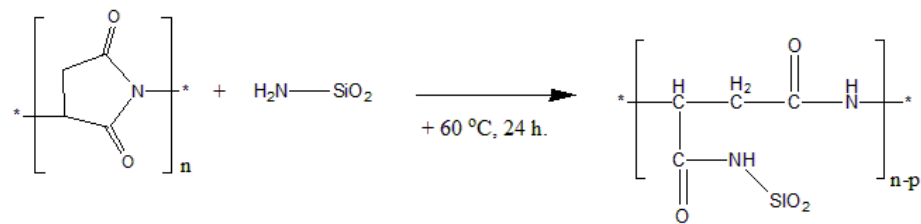


Cysteamine modified polyaspartic acid

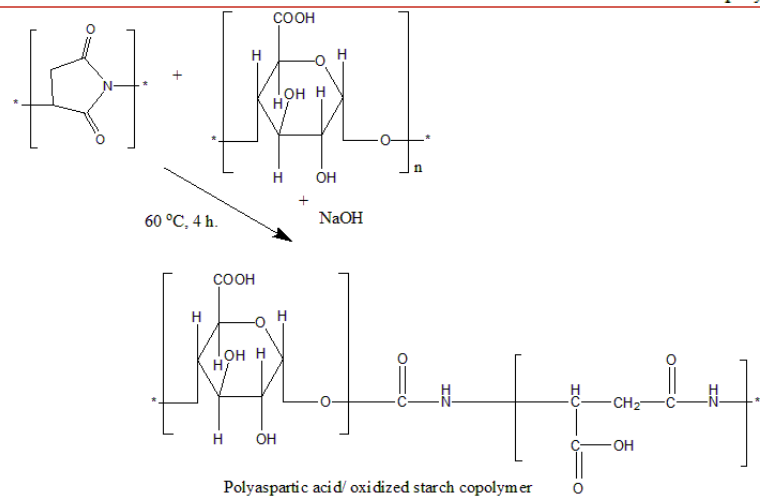


Polyaspartic acid/urea graft copolymer

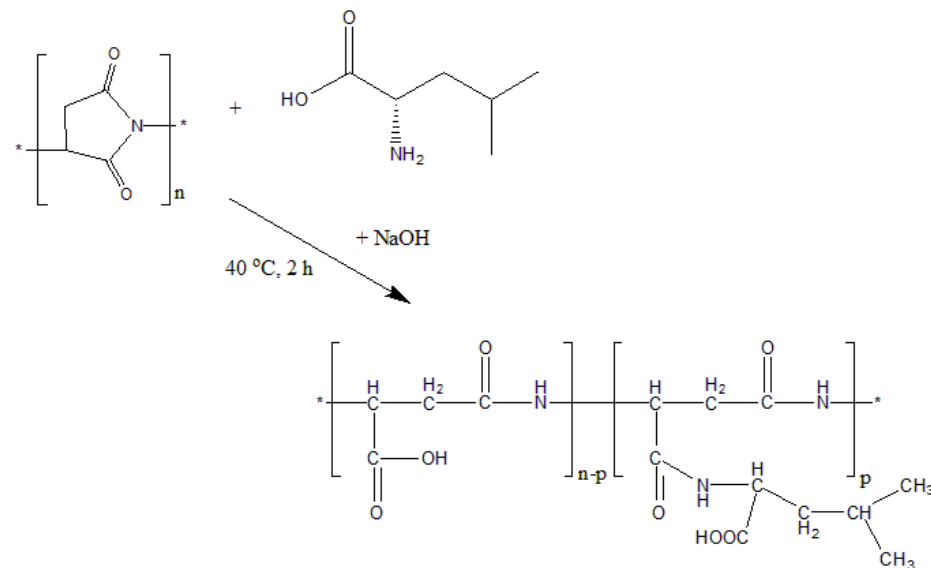
Figure 2 Synthesis schemes of modified PSI [3, 32, 34].



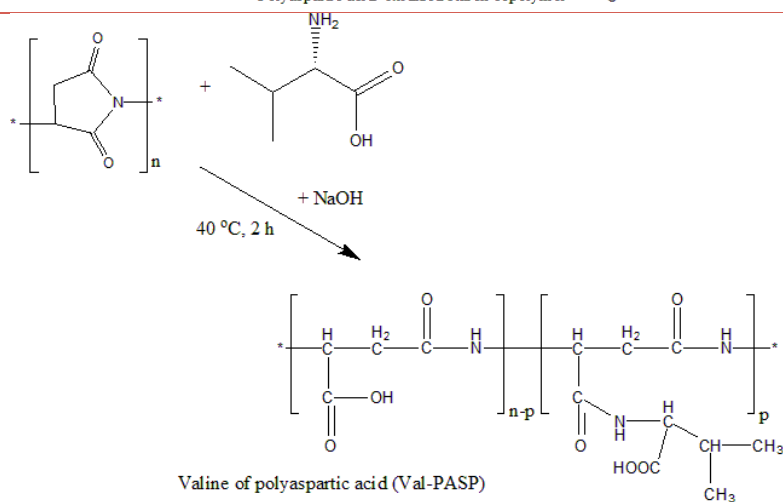
Nanosilica modified with polyaspartic acid



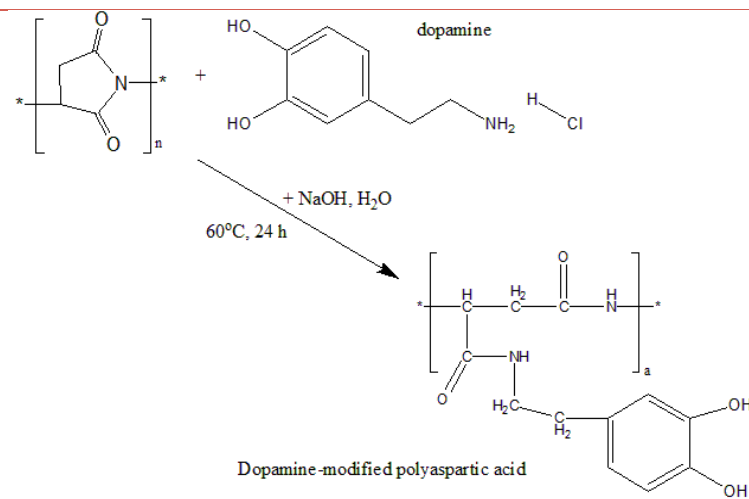
Polyaspartic acid/ oxidized starch copolymer



Leucine of poly aspartic acid (Leu-PASP)



Valine of polyaspartic acid (Val-PASP)



Dopamine-modified polyaspartic acid

Figure 3 Synthesis schemes of modified PSI (Continued) [20, 31, 35, 40, 42, 43].



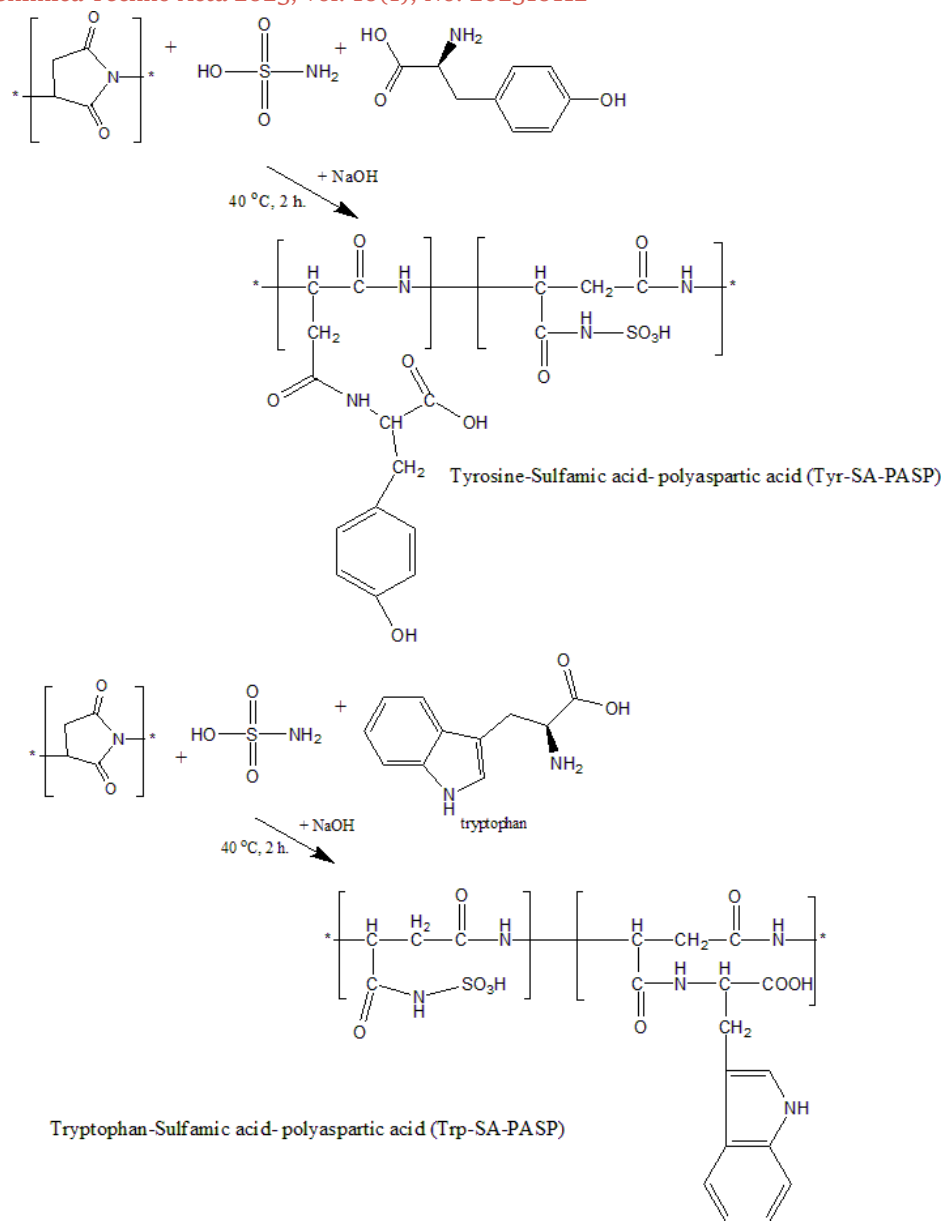
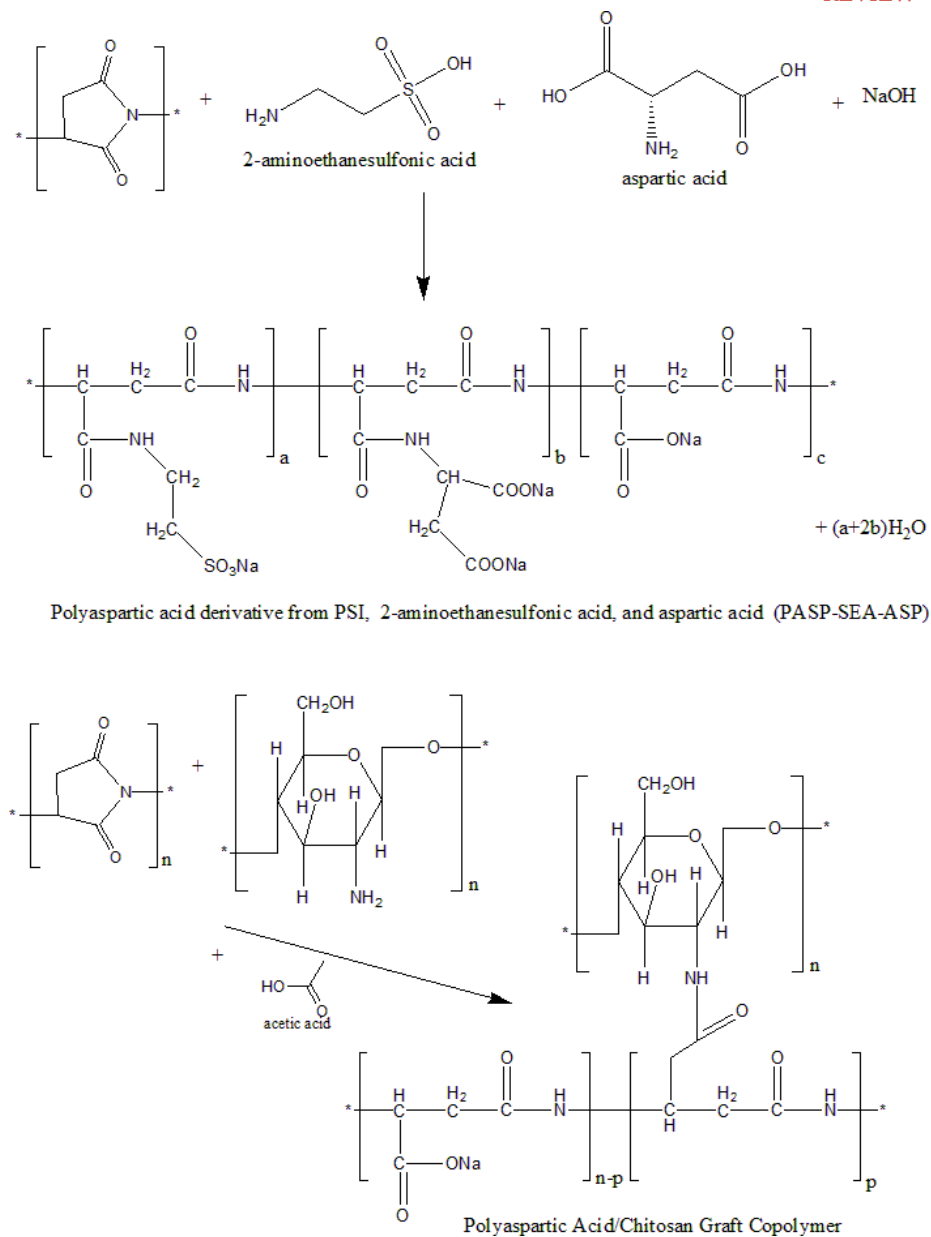


Figure 4 Synthesis schemes of modified PSI (Continued) [38, 39, 44].



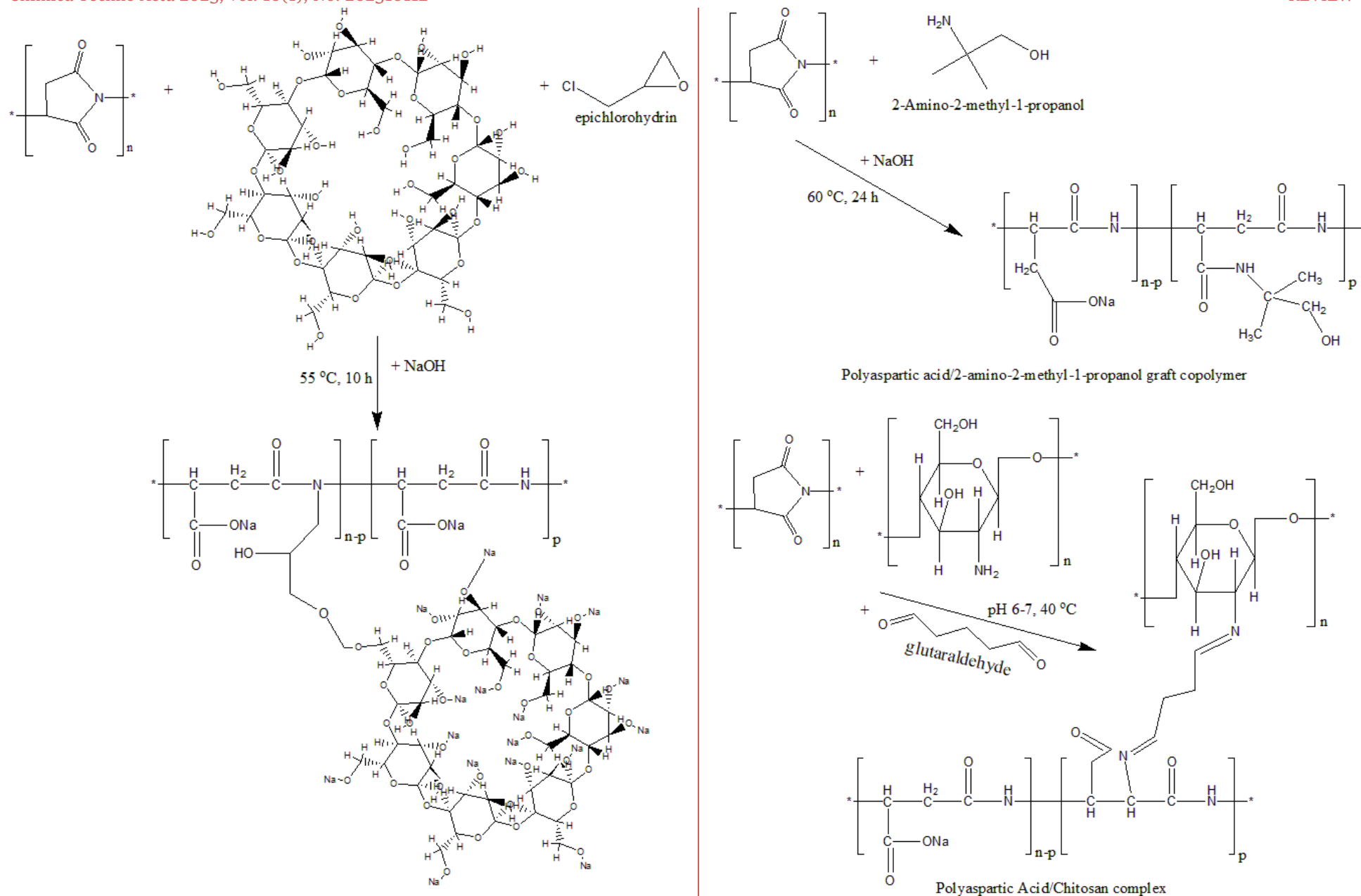
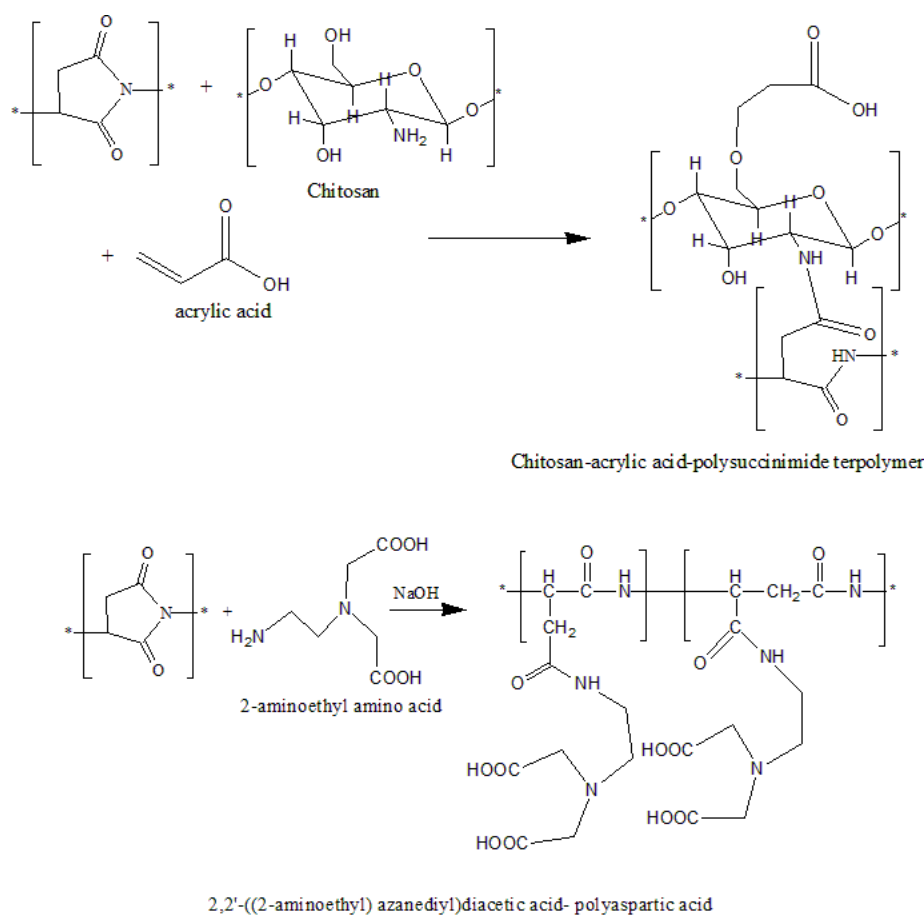


Figure 5 Synthesis schemes of modified PSI [23, 27, 45].





**Figure 6** Synthesis schemes of modified PSI [22, 46].

Both weight loss and electrochemical methods (potentiodynamic polarization and EIS) are used to determine corrosion rate and inhibition efficiency. The weight loss method investigates the inhibition efficiency by the difference in metal mass before and after tests. Traces of corrosion on the metal surface can be observed through this method. It is often combined with the scanning electron microscope for more detailed information. Electrochemical impedance spectroscopy (EIS) is conducted to obtain information about kinetics and inhibitor adsorption through charge transfer and double-layer thickness at the metal-inhibitor interface [48, 49]. The increase in inhibition efficiency is caused by increasing charge transfer resistance and decreasing electric double-layer capacitance. Charge transfer resistance reflects electrons, Fe ions, and corrosive ion movements in the corroded system. Greater charge transfer resistance decreases the motions of electrons, Fe ions, and corrosive ions in the solution phase. Therefore, the corrosion rate is slowed down. At the same time, electric double-layer capacitance corresponds to the thickness of the electric double-layer after water molecules are replaced by inhibitors [49]. The presence of modified PSI on the metal surface reduces the dielectric constant of the corroded system. It is followed by the reduction of electric double-layer capacitance. Then, the potentiodynamic polarization test is carried out to determine the type of inhibitor or inhibition mechanism, such as cathodic, anodic, or mixed-type inhibitor.

The increase in immersion time can increase or decrease corrosion inhibition efficiency. It depends on the protective film properties from modified PSI formed on the metal surface. This film formation is affected by adsorption and chemical reaction rates between metal and corrosion inhibitors. This film's breaking down and reestablishing can also occur during immersion [44]. Polyaspartic acid + Zn ion was found to be a good corrosion inhibitor for long-time protection. It can maintain steel inhibition performance near 100% after 168 hours of exposure.

Inhibition efficiency is also influenced by temperature. Modified PSI that is physically adsorbed on the metal surface can be released from the surface at higher temperatures [50]. Besides that, electrochemical reactions in the corroded metal will be accelerated. From the literature study, the highest inhibition efficiency of modified PSI was achieved at 25 or 35 °C. It shows that the interactions between inhibitor molecules and metals are dominated by physical adsorption. Corrosion inhibitors do not directly participate in electrochemical reactions on the metal surface. However, their existence in the metal/solution interface affects all electrochemical reactions, including the diffusion of corrosive species from the solution phase to the metal surface. Increasing inhibitor concentration would expand the inhibitor's surface coverage, forming a thin protective film on the metal surface and improving the corrosion inhibition efficiency.

**Table 1** Corrosion inhibition performance of PASP, oligomer form, and modified PSI.

No.	Inhibitor name	Metal/alloy and corrosive media	Optimum condition and maximum efficiency	Ref.
1a	Polyaspartic acid + Zn ion	Mild steel in aerated NaCl 3.0% solution	Weight loss 1000.0 mg·L <sup>-1</sup> for PASP + 10 mg·L <sup>-1</sup> Zn ion; 25, 30, 35 °C; 168 hours IE ≈ 100.0% PDP	[36]
			1000.0 mg·L <sup>-1</sup> for PASP + 10 mg·L <sup>-1</sup> for Zn ion; 35 °C; stirring speed = 650 rpm. IE = 99.0% EIS 1000.0 mg·L <sup>-1</sup> for PASP + 10 mg·L <sup>-1</sup> for Zn ion; 35 °C; stirring speed = 650 rpm. IE = 95.2%	
1b	Polyaspartic acid		Weight loss 2000.0 mg·L <sup>-1</sup> ; 25 °C; 168 hours IE = 61.0% PDP	
			2000.0 mg·L <sup>-1</sup> ; 35 °C; stirring speed = 650 rpm. IE = 63.0% EIS 2000.0 mg·L <sup>-1</sup> ; 35 °C; stirring speed = 650 rpm. IE = 86.40%	
2a	Polyaspartic acid/chitosan complex	A3 carbon steel in NaCl 3.5% solution	Weight loss 8 mg·L <sup>-1</sup> ; 45±1 °C; 72 hours, rotating speed = 75 rpm IE = 83.50% PDP 20 mg·L <sup>-1</sup> ; 25 °C IE = 87.56% EIS	[45]
			20 mg·L <sup>-1</sup> ; 25 °C IE = 86.01%	
2b	Polyaspartic acid		Weight loss 8 mg·L <sup>-1</sup> ; 45±1 °C; 72 hours, rotating speed = 75 rpm IE = 58.80%	
3a	Cysteamine modified polyaspartic acid	Mild steel in 0.5 M H <sub>2</sub> SO <sub>4</sub>	Weight loss 100 mg·L <sup>-1</sup> ; 25 °C; 12 hours IE = 93.90% PDP 100 mg·L <sup>-1</sup> ; 25 °C; 1 hour IE = 96.50% EIS	[3]
			100 mg·L <sup>-1</sup> ; 25 °C; 1 hour IE = 92.90%	
3b	Polyaspartic acid		Weight loss 100 mg·L <sup>-1</sup> ; 25 °C; 12 hours IE = 67.50%	
4a	Dopamine-modified polyaspartic acid	Mild steel in 0.5 M H <sub>2</sub> SO <sub>4</sub>	Weight loss 200 mg·L <sup>-1</sup> ; 25 °C; 12 hours IE = 91.20% PDP 200 mg·L <sup>-1</sup> ; 25 °C; 1 hour IE = 92.90% EIS	[40]
			200 mg·L <sup>-1</sup> ; 25 °C; 1 hour IE = 88.40%	
4b	Polyaspartic acid		PDP 200 mg·L <sup>-1</sup> ; 25 °C; 1 hour IE = 77.50% EIS 200 mg·L <sup>-1</sup> ; 25 °C; 1 hour IE = 79.30%	

**Table 2** Performance of PASP and modified PSI as scale inhibitors.

No.	Inhibitor name	Scale types	Experimental condition and efficiency	Ref.
1	Polyaspartic acid/ diethylenetriamine graft copolymer	CaCO <sub>3</sub> and Ca <sub>3</sub> (PO <sub>4</sub> ) <sub>2</sub>	- CaCO <sub>3</sub> : 6 mg·L <sup>-1</sup> , ≤80 °C, pH 5-9, IE ≈ 99.9%; - Ca <sub>3</sub> (PO <sub>4</sub> ) <sub>2</sub> : 15 mg·L <sup>-1</sup> , ≤80 °C, pH 5-9, IE ≈ 99.9%;	[32]
2	Polyaspartic acid-serine grafted copolymer	CaCO <sub>3</sub> , Ca <sub>3</sub> (PO <sub>4</sub> ) <sub>2</sub> , and CaSO <sub>4</sub>	- CaCO <sub>3</sub> : 5 mg·L <sup>-1</sup> , 80 °C, pH 9, 10 hours, IE ≈ 100%; - CaSO <sub>4</sub> : 5 mg·L <sup>-1</sup> , 80 °C, pH 9, 10 hours, IE ≈ 100%; - Ca <sub>3</sub> (PO <sub>4</sub> ) <sub>2</sub> : 22 mg·L <sup>-1</sup> , 80 °C, pH 9, 10 hours, IE ≈ 100%;	[51]
3	Poly(aspartic acid)-tryptophan grafted copolymer	CaCO <sub>3</sub> and CaSO <sub>4</sub>	- CaCO <sub>3</sub> : 4 mg·L <sup>-1</sup> , 80 °C, 8 hours, IE = 96% - CaSO <sub>4</sub> : 0.4 mg·L <sup>-1</sup> , 70 °C, 8 hours, IE = 90%	[31]
4a	Polyaspartic acid/urea graft copolymer	CaCO <sub>3</sub> , Ca <sub>3</sub> (PO <sub>4</sub> ) <sub>2</sub> , and CaSO <sub>4</sub>	- CaCO <sub>3</sub> : 10 mg·L <sup>-1</sup> , 80 °C, pH 9, 8 hours, IE ≈ 93%; - CaSO <sub>4</sub> : 4 mg·L <sup>-1</sup> , 80 °C, pH 9, 8 hours, IE ≈ 97%; - Ca <sub>3</sub> (PO <sub>4</sub> ) <sub>2</sub> : 12 mg·L <sup>-1</sup> , 80 °C, pH 9, 8 hours, IE ≈ 100%;	[35]
4b	Polyaspartic acid		- CaCO <sub>3</sub> : 10 mg·L <sup>-1</sup> , 80 °C, pH 9, 8 hours, IE ≈ 63%; - CaSO <sub>4</sub> : 4 mg·L <sup>-1</sup> , 80 °C, pH 9, 8 hours, IE ≈ 82%; - Ca <sub>3</sub> (PO <sub>4</sub> ) <sub>2</sub> : 12 mg·L <sup>-1</sup> , 80 °C, pH 9, 8 hours, IE ≈ 72%;	
5	Poly(aspartic acid-citric acid) copolymer	Ca <sub>3</sub> (PO <sub>4</sub> ) <sub>2</sub>	- 8 mg·L <sup>-1</sup> , 80 °C, 10 hours, pH 9, IE ≈ 63%;	[52]
6a	Tyrosine-sulfamic acid-polyaspartic acid (Tyr-SA-PASP)	CaSO <sub>4</sub>	- 4.0 mg·L <sup>-1</sup> , 80 °C, 10 hours, pH 7, IE ≈ 98%;	[38]
6b	Tryptophan-sulfamic acid-polyaspartic acid (Trp-SA-PASP)		- 5.0 mg·L <sup>-1</sup> , 80 °C, 10 hours, pH 7, IE ≈ 98%;	
6c	Polyaspartic acid		- 5.0 mg·L <sup>-1</sup> , 80 °C, 10 hours, pH 7, IE ≈ 90%;	
7a	Polyaspartic acid-capped aminomethylene phosphonic acid	CaCO <sub>3</sub> and BaSO <sub>4</sub>	- CaCO <sub>3</sub> : 2 ppm, 130 °C, 7 days, pH 4-6, IE = -; - BaSO <sub>4</sub> : 20 ppm, 130 °C, 7 days, pH 4-6, IE = -;	
7b	Polyaspartic acid-capped bisphosphonic acid	CaCO <sub>3</sub> and BaSO <sub>4</sub>	- CaCO <sub>3</sub> : 2 ppm, 130 °C, 7 days, pH 4-6, IE = -; - BaSO <sub>4</sub> : 20 ppm, 130 °C, 7 days, pH 4-6, IE = -;	
7c	Polyaspartic acid-capped aminomethanesulfonic acid	CaCO <sub>3</sub> and BaSO <sub>4</sub>	- CaCO <sub>3</sub> : 5 ppm, 130 °C, 7 days, pH 4-6, IE = -; - BaSO <sub>4</sub> : 20 ppm, 130 °C, 7 days, pH 4-6, IE = -;	[1]
7d	Polyaspartic acid-capped aminomethanesulfonic acid	CaCO <sub>3</sub> and BaSO <sub>4</sub>	- CaCO <sub>3</sub> : 5 ppm, 130 °C, 7 days, pH 4-6, IE = -; - BaSO <sub>4</sub> : 20 ppm, 130 °C, 7 days, pH 4-6, IE = -;	
7e	Polyaspartic acid	CaCO <sub>3</sub> and BaSO <sub>4</sub>	- CaCO <sub>3</sub> : 100 ppm, 130 °C, 7 days, pH 4-6, IE = -; - BaSO <sub>4</sub> : 50 ppm, 130 °C, 7 days, pH 4-6, IE = -;	
8a	Polyaspartic acid/ oxidized starch copolymer	CaCO <sub>3</sub> and CaSO <sub>4</sub>	- CaCO <sub>3</sub> : 8 mg·L <sup>-1</sup> , 80 °C, 10 hours, pH 7, IE ≈ 100%; - CaSO <sub>4</sub> : 10 mg·L <sup>-1</sup> , 70 °C, 10 hours, IE ≈ 100%;	[20]
8b	Polyaspartic acid		- CaCO <sub>3</sub> : 8 mg·L <sup>-1</sup> , 80 °C, 10 hours, pH 7, IE = 97.1%; - CaSO <sub>4</sub> : 16 mg·L <sup>-1</sup> , 70 °C, 10 hours, IE ≈ 100%;	
9a	Nanosilica modified with polyaspartic acid	CaCO <sub>3</sub> and CaSO <sub>4</sub>	- CaCO <sub>3</sub> : 50 mg·L <sup>-1</sup> , 80 °C, 10 hours, IE ≈ 70%; - CaSO <sub>4</sub> : 6 mg·L <sup>-1</sup> , 70 °C, 10-25 hours, IE ≈ 100%;	[42]
9b	Polyaspartic acid		- CaCO <sub>3</sub> : 50 mg·L <sup>-1</sup> , 80 °C, 8 hours, IE ≈ 50%; - CaSO <sub>4</sub> : 6 mg·L <sup>-1</sup> , 70 °C, <5 hours, IE ≈ 100%;	
10a	Ring-opening graft modification of polyaspartic acid (Polyaspartic acid- aspartic acid, and monoethanolamine)	CaCO <sub>3</sub> and Ca <sub>3</sub> (PO <sub>4</sub> ) <sub>2</sub>	- CaCO <sub>3</sub> : 4 mg·L <sup>-1</sup> , 80 °C, 10 hours, pH 9, IE ≈ 100%; - Ca(PO <sub>4</sub> ) <sub>4</sub> : 4 mg·L <sup>-1</sup> , 80 °C, 10 hours, pH 9, IE ≈ 100%;	[34]
10b	Polyaspartic acid	CaCO <sub>3</sub> and Ca <sub>3</sub> (PO <sub>4</sub> ) <sub>2</sub>	- CaCO <sub>3</sub> : 4 mg·L <sup>-1</sup> , 80 °C, 10 hours, pH 9, IE ≈ 93%; - Ca(PO <sub>4</sub> ) <sub>4</sub> : 4 mg·L <sup>-1</sup> , 80 °C, 10 hours, pH 9, IE ≈ 80%;	
11	2,2'-((2-aminoethyl)azanediyl)diacetic acid-polyaspartic acid	CaCO <sub>3</sub> and CaSO <sub>4</sub>	- CaCO <sub>3</sub> : 50 mg·L <sup>-1</sup> , 70 °C, 8 hours, IE ≈ 70%; - CaSO <sub>4</sub> : 5 mg·L <sup>-1</sup> , 70 °C, 10-24 hours, IE ≈ 100%.	[46]

\* - : not mentioned.

## 4.2. Scale inhibitor

Static scale inhibition tests generally analyze the performance of modified PSI as scale inhibitors. Actually, PASP can decrease scale formation in all experimental conditions. However, advanced modifications of PSI exhibit better scale inhibition ability in several concentrations,

scale types, pH, temperatures, and testing times. It corresponds to the extra-functional groups, for instance, hydroxyl, amine, amides, ether, acylamino, amino sulfonic acid, aromatic ring, or carboxyl, forming coordination bonds with calcium or barium cations. Thereby, interactions of those cations with anions (CO<sub>3</sub><sup>2-</sup>, SO<sub>4</sub><sup>2-</sup>, and PO<sub>4</sub><sup>3-</sup>) will be inhibited. Meanwhile, different synthesis routes of

PSI lead to disparity in the scale inhibition performance of PASP and other modified PSI [31]. The inhibition efficiency of modified PSI could reach 100% in small concentrations.

The scale types show different inhibition efficiency of modified PSI, although the experiment is carried out at the same concentration, temperature, pH, and testing time. The increase in inhibitor concentration can increase scale inhibition efficiency. It is related to the presence of more crystal nucleation barriers in the solution. On the contrary, the increase of calcium/barium ion concentrations will decrease the efficiency of the inhibitor because collision probability among calcium or barium ions and  $\text{CO}_3^{2-}$ ,  $\text{SO}_4^{2-}$ , or  $\text{PO}_4^{3-}$  will increase [35].

The performance of scale inhibitors depends on the system temperature. Higher temperature supports decreasing the crystal nucleus's adsorption capacity to accelerate scale nucleation [53, 54]. Dispersion of scales will reduce when the temperature is higher than room temperature [35]. Besides that, the reduction of inhibition efficiency at higher temperatures is also caused by the gradual degradation of inhibitor compounds that are not heat resistant [32]. Thus, the performance of inhibitors will be restricted. However, tyrosine-sulfamic acid-polyaspartic acid still has high  $\text{CaSO}_4$  scale inhibition efficiency at increased temperatures [38]. This indicates its resilience toward the temperature effect.

Testing time also influences the scale inhibitor performance. It corresponds to the crystal formation, which will rise over time. Great endurance scale inhibitors have long-term interaction/bond stability between functional groups of inhibitor and earth-alkaline ions ( $\text{Ca}^{2+}$  or  $\text{Ba}^{2+}$ ) [42]. Scale inhibition of 2,2'-((2-aminoethyl)azanediyl) diacetic acid toward  $\text{CaSO}_4$  could be maintained near 100% at a range of 1–24 hours [46].

The increase of  $\text{pH} > 10$  causes a reduction of inhibition efficiency due to increasing hydroxyl ion concentration in the solution [55]. Consequently, scales are more easily deposited [20]. Typically, for the  $\text{Ca}_3(\text{PO}_4)_2$  scale, polyaspartic acid/diethylenetriamine graft copolymer's inhibition efficiency decreases with rising pH. More phosphate ions are available to form  $\text{Ca}_3(\text{PO}_4)_2$  precipitate at higher pH.  $\text{H}(\text{PO}_4)^{2-}$  and  $\text{H}_2(\text{PO}_4)^-$  are formed at low pH. These ions can dissolve better in water [32].

In the same concentration and conditions, a combination of grafted copolymers and  $\text{Ca}^{2+}$  ions is easier to adsorb on the scale crystal surface than a non-grafted polymer [56]. Adsorbed inhibitors on the scale crystals/crystal nuclei can enlarge crystal damage resulting the irregular shapes [32]. Meanwhile, intramolecular hydrogen bonding in heterocyclic compounds increases the ability of the inhibitor to inhibit  $\text{Ca}_3(\text{PO}_4)_2$  scale formation [32].

### 4.3. Corrosion and scale inhibitor

Table 3 displayed the performance of OSI and modified PSI as corrosion and scale inhibitors. Seawater was used as a testing solution because it contains many ions like  $\text{Na}^+$ ,  $\text{Cl}^-$ ,

$\text{Ca}^{2+}$ ,  $\text{HCO}_3^-$ , and  $\text{SO}_4^{2-}$  as corrosive species and triggers of scale formation.  $\text{CO}_2$ -saturated NaCl solution can also be applied as an alternative solution. The usability expansion of this compound is an advantage. Good scale and corrosion inhibitors afford high inhibition efficiency to prevent corrosion reaction and scale formation. OSI and modified PSI perform better as corrosion and scale inhibitors than PASP. The increase in concentration generally increases inhibition efficiency (IE).

Moreover, the inhibition efficiency of several modified PSI reached 100%. However, the relative inhibition efficiency decreases with increasing temperature. Meanwhile, oligosuccinimide has moderate corrosion and scale inhibition efficiency [29, 41]. OSI is not combined with other substances to form copolymers or composites. Thus, no additional functional groups and multiple bonds can upgrade its performance. However, OSI does not require advanced modification because it already has good water solubility. Economically, this inhibitor is more efficient in the fabricating process.

PASP is the simplest form of modified PSI. The presence of the carboxylic groups in a PASP molecule acts as a chelating and dispersing agent for scales [57]. However, PASP needs modifications to increase its performance by adding functional groups such as hydroxyl, amino, sulfonic, or extra carboxylic groups. Those groups affect adsorption and the complexation ability of PSI to  $\text{Ca}^{2+}$  ions owing to the abundance of lone pair electrons. Thereby, the nucleation rate of crystal growth will be reduced [31]. Then, modified PSI can deform the crystal lattice of scale sources. Besides that, it can fix the utilization of PSI as corrosion and scale inhibitors at higher temperatures and more extended contact periods [31, 51]. Meanwhile, the polymerization time and molecular weight of a PSI/PASP also influence scale inhibition [58].

Classification of inhibitor type (anodic, cathodic, or mixed type) is summarized in Table 4. Various types of inhibitors are based on corrosion potential shifts toward blank potential. Corrosion potential is determined from Tafel extrapolation. The increase in polarization curves slope also increases polarization resistance as well as the inhibition ability of the inhibitor [45]. PASP was generally categorized as a mixed-type inhibitor, predominantly as an anodic inhibitor under certain conditions [44, 59]. As the anodic inhibitor, the slope anode curve changes significantly more than the cathode curve.

## 5. Scale-inhibition mechanism

There are several general stages of scale formation: (1) formation and pairing of alkaline earth cations and anions ( $\text{CO}_3^{2-}$ ,  $\text{SO}_4^{2-}$ ,  $\text{PO}_4^{3-}$ ); (2) formation of micro-aggregates; (3) nucleation to form microcrystals; (4) crystal growth to form macro crystals; and (5) incorporation of macrocrystal to form deposits/scales [60].

**Table 3** Performance of OSI and modified PSI as corrosion and scale inhibitors.

No.	Inhibitor name	Metal/alloy and corrosive media	Optimum condition and efficiency (corrosion inhibition)	Scale types	Optimum condition and efficiency (scale inhibition)	Ref.
1	Modified PSI from PSI, 2-aminoethanesulfonic acid, and aspartic acid (PASP-SEA-ASP)	A3 carbon steel in seawater	Weight loss - 100 mg·L <sup>-1</sup> ; 40 °C; 72 hours; stirring speed = 75 rpm, IE = 97.0% PDP - 100 mg·L <sup>-1</sup> ; 72 hours; IE = 43.98%	Seawater with calcium ions	14 mg·L <sup>-1</sup> , 80 °C, IE ≈ 100%	[44]
2a	Polyaspartic acid/chitosan graft copolymer	Carbon steel in 3.5% NaCl solution	Weight loss - 25 mg·L <sup>-1</sup> ; 45 °C; 75 rpm, 72 hours, IE = 82% PDP - 30 mg·L <sup>-1</sup> ; 25 °C, IE = 82.57% EIS - 30 mg·L <sup>-1</sup> ; 25 °C, IE = -	CaCO <sub>3</sub> , and Ca <sub>3</sub> (PO <sub>4</sub> ) <sub>2</sub>	- CaCO <sub>3</sub> : 8 mg·L <sup>-1</sup> , 80 °C, 10 hours, pH 9, IE ≈ 92% - Ca(PO) <sub>4</sub> : 8 mg·L <sup>-1</sup> , 80 °C, 10 hours, pH 9, IE ≈ 89%	[39]
2b	Polyaspartic acid		Weight loss - 35 mg·L <sup>-1</sup> , 45 °C, 75 rpm, 72 hours, IE ≈ 60%	CaCO <sub>3</sub> , and Ca <sub>3</sub> (PO <sub>4</sub> ) <sub>2</sub>	- CaCO <sub>3</sub> : 8 mg·L <sup>-1</sup> , 80 °C, 10 hours, pH 9, IE ≈ 68% - Ca(PO) <sub>4</sub> : 8 mg·L <sup>-1</sup> , 80 °C, 10 hours, pH 9, IE ≈ 46%	
3	Glycine of polyaspartic acid (Gly-PASP)	X - 65 type carbon steel in artificial seawater	PDP - 250 mg·L <sup>-1</sup> ; 25 °C, IE = 83.1% EIS - 250 mg·L <sup>-1</sup> ; 25 °C, IE = 83.8%	CaSO <sub>4</sub>	125 mg·L <sup>-1</sup> , 90 °C, 24 hours, IE = 90.2%	[33]
4a	Polyaspartic acid/2-amino-2-methyl-1-propanol graft copolymer	Carbon steel	Weight loss - 24 mg·L <sup>-1</sup> ; 45±1 °C; 75 rpm, 72 hours IE = 28%	CaCO <sub>3</sub> , CaSO <sub>4</sub> , and Ca <sub>3</sub> (PO <sub>4</sub> ) <sub>2</sub>	- CaCO <sub>3</sub> : 1 mg·L <sup>-1</sup> , 80 °C, 6-16 hours, IE ≈ 100% - CaSO <sub>4</sub> : 4 mg·L <sup>-1</sup> , 80 °C, 6 hours, IE ≈ 100% - Ca(PO) <sub>4</sub> : 14 mg·L <sup>-1</sup> , 80 °C, 10 hours, IE ≈ 100%	[27]
4b	Polyaspartic acid	Carbon steel	Weight loss - 24 mg·L <sup>-1</sup> ; 45±1 °C; 75 rpm, 72 hours IE = 21%	CaCO <sub>3</sub> , CaSO <sub>4</sub> , and Ca <sub>3</sub> (PO <sub>4</sub> ) <sub>2</sub>	- CaCO <sub>3</sub> : 1 mg·L <sup>-1</sup> , 80 °C, 6-16 hours, IE ≈ 100% - CaSO <sub>4</sub> : 4 mg·L <sup>-1</sup> , 80 °C, 6 hours, IE ≈ 90% - Ca <sub>3</sub> (PO) <sub>4</sub> : 14 mg·L <sup>-1</sup> , 80 °C, 10 hours, IE ≈ 30%	
5a	Valine of polyaspartic acid (Val-PASP)	Carbon steel in seawater	PDP - 250 mg·L <sup>-1</sup> ; room temperature; 1 hour, IE = 86.94% EIS - 250 mg·L <sup>-1</sup> ; room temperature; 1 hour, IE = 87.0%	CaSO <sub>4</sub>	125 mg·L <sup>-1</sup> , 90 °C, 24 hours, IE = 92.3%	[43]
5b	Leucine of polyaspartic acid (Leu-PASP)		PDP - 250 mg·L <sup>-1</sup> ; room temperature; 1 hour, IE = 88.62% EIS - 250 mg·L <sup>-1</sup> ; room temperature; 1 hour, IE = 88.69%		125 mg·L <sup>-1</sup> , 90 °C, 24 hours, IE = 94.1%	
6	Polyaspartic acid grafted β-cyclodextrin	N80 carbon steel in artificial seawater	Weight loss - 800 mg·L <sup>-1</sup> , 60 °C, 72 hours IE = 68.4% PDP - 25 °C; 1 hour, IE = -	CaCO <sub>3</sub> , CaSO <sub>4</sub>	- CaCO <sub>3</sub> : IE ≈ 77.4% - CaSO <sub>4</sub> : IE ≈ 94.6%	[23]
7	Chitosan-acrylic acid-polysuccinimide terpolymer	3.5% NaCl	EIS - 500 mg·L <sup>-1</sup> , IE = 71.17%	CaCO <sub>3</sub>	125 mg·L <sup>-1</sup> , IE = 87.96%	[22]
8	Oligosuccinimide	Carbon steel in CO <sub>2</sub> -Saturated 1% NaCl Solution	Weight loss - 100 mg·L <sup>-1</sup> ; 35 °C; 48 hours, IE = 45.37% PDP - 92.5 mg·L <sup>-1</sup> ; 25 °C; 30 min, IE = 62.73% EIS - 92.5 mg·L <sup>-1</sup> ; 25 °C; 30 minutes, IE = 62.71%	CaCO <sub>3</sub> , CaSO <sub>4</sub>	- CaCO <sub>3</sub> : 10 mg·L <sup>-1</sup> , 80 °C, 24 hours, IE ≈ 73.2% - CaSO <sub>4</sub> : 10 mg·L <sup>-1</sup> , 80 °C, 24 hours, IE ≈ 55.3%	[29, 41]

\* - : not mentioned.



Stages 1–2 are related to the supersaturation events that temperature and pressure influence [61]. Nucleation is marked by the formation of microparticles after random cation-anion collision [62]. The scale inhibitors in the brine solution system can interfere with one or more stages of scale formation. Meanwhile, modified PSI is more amorphous than pure PASP [34]. Thus, the crystallinity of scales reduces with time [38]. In other words, scale crystals tend to be amorphous. Coordination bonds between calcium ions ( $\text{Ca}^{2+}$ ) and heteroatoms in functional groups of scale inhibitors induce morphology changes due to defects of microcrystalline structures [5]. The functional groups and lone pair electrons act as adsorption agents on scale crystals to prevent crystal growth [20].

Furthermore, functional groups with similar charges cover the microcrystals and create the repulsion phenomenon between two or more covered microcrystals [52]. Thereby, crystal solubilization is maintained in the brine solution. Besides that, the change in microcrystal morphology changes the shape of the macrocrystal to prevent the build-up of regular crystalline lattice [60].

## 6. Adsorption study oligosuccinimide and modified PSI

The adsorption isotherm describes the interactions of metal surfaces with OSI and modified PSI as corrosion inhibitors. Several types of adsorption isotherms, such as Temkin, Frumkin, and Langmuir adsorption isotherms, are generally tested to get information about the behavior-suitability of molecular inhibitors on the metal surface. These isotherms correlate surface coverage and inhibitor concentration. The conclusion depends on the linear correlation coefficient value (close to 100). From this review, oligosuccinimide, dopamine-modified polyaspartic acid, and cysteamine-modified polyaspartic acid obeyed Langmuir adsorption isotherm. It means those modified PSI occupy specific sites, then form a protective monolayer on the surface area. Substitution of functional groups in the PSI/PASP also affects adsorption on the scales and inhibition efficiency [63].

Furthermore, there are adsorption energy and adsorption type to clarify the inhibition mechanism of modified PSI as corrosion inhibitors. Adsorption energy leads to the ease of inhibitor molecules to adsorb on the metal surface. A corrosion inhibitor that is readily adsorbed has a more negative adsorption energy value. This adsorption energy is usually represented by the standard Gibbs free energy of the adsorption ( $\Delta G^{\circ}_{ads}$ ). Then, the adsorption type of inhibitor (physisorption, chemisorption, or semi-physisorption/chemisorption) is determined by a value of released energy ( $\Delta G^{\circ}_{ads}$ ). The chemisorption of an inhibitor to a metal surface depends on the polarity of functional groups. These groups provide electron pairs to form complexes with metal [64].

–  $\Delta G^{\circ}_{ads} < 20 \text{ kJ}\cdot\text{mol}^{-1}$  is physisorption;

–  $20 < \Delta G^{\circ}_{ads} < 40 \text{ kJ}\cdot\text{mol}^{-1}$  is semi chemisorption;

–  $\Delta G^{\circ}_{ads} > 40 \text{ kJ}\cdot\text{mol}^{-1}$  is chemisorption [65].

## 7. Biodegradation performance of modified PSI

According to the Convention for the Protection of the Marine Environment of the North-East Atlantic, a scale inhibitor is categorized as a green scale inhibitor if the biodegradation rate is more than 60% within 28 days [66]. It is based on the Biochemical Oxygen Demand (BOD) parameter. Not only that,  $\text{LC}_{50}$  and  $\text{EC}_{50}$  must be greater than  $10 \text{ mg}\cdot\text{L}^{-1}$  from a toxicity test [1]. Table 5 displays the biodegradation performance of three modified PSI. It shows that polyaspartic acid has a faster biodegradation rate (>80%). Larger molecules in modified PSI affect this condition. However, biodegradation rates of modified PSI are still conform to the international standards for green corrosion and scale inhibitors.

## 8. Computational quantum study of modified PSI

A computational chemistry study of modified PSI was conducted to get the information about their theoretical activity as corrosion and scale inhibitors. Molecular structure influences the chemical reactivity of inhibitors. Quantum chemical calculations are applied to obtain the appropriate results. Because of huge molecules, a computational chemical method to calculate the parameters of modified PSI generally is semi-empirical. Another method was carried out by density functional theory (DFT), for example, for the cysteamine-modified polyaspartic acid. Important parameters that specify corrosion inhibition capability are HOMO and LUMO orbitals energy [67, 68]. These parameters are used to determine theoretical parameters such as energy gap ( $\Delta E$ ), hardness ( $\eta$ ), electronegativity ( $\chi$ ), and the fraction of transferred electron ( $\Delta N$ ) from the inhibitor molecules to the metal.

Adsorption of inhibitor molecules to the metal is affected by HOMO and LUMO orbitals [69]. Greater HOMO and LUMO energies produce greater inhibition efficiency. Inhibitor molecules are easier to share their lone electron pair at higher HOMO energy or difficult to accept electron pair at high LUMO energy [70, 71]. The gap between LUMO and HOMO is the band gap energy. Reactive inhibitors have a small band gap energy [72]. Then, inhibitor molecules with smaller band gaps facilitate the excitation of the electron. Thus, chemical reactions occur quickly. Modified PSI with aromatic rings has HOMO orbitals that strongly interact with the metallic orbitals generating chemical adsorption [73]. The density of  $\pi$  electrons is easily submitted from the inhibitor HOMO orbital to the metal LUMO orbital with electronic delocalization in the aromatic rings [69]. Electronegativity ( $\chi$ ) is related to the convenience of atom/ion/molecule for attracting electrons.

**Table 4** Annotations of adsorption energy, adsorption type, adsorption isotherm, and inhibitor type on modified PSI, including OSI as a corrosion inhibitor.

No	Corrosion inhibitor	Adsorption energy and adsorption type	Adsorption isotherm	Type of inhibitor	Ref.
1	Modified polyaspartic acid derivative (polysuccinimide + 2-aminoethanesulfonic + aspartic acid)	-	-	Anodic type inhibitor	[44]
2	Polyaspartic acid/chitosan graft copolymer	-	-	Anodic type inhibitor	[39]
3	Glycine of polyaspartic acid (Gly-PASP)	-	-	Mixed-type inhibitor, a predominantly anodic inhibitor	[33]
4	Valine of polyaspartic acid (Val-PASP)	-	-	Mixed-type inhibitor, a predominantly anodic inhibitor	[43]
5	Leucine of polyaspartic acid (Leu-PASP)	-	-	Mixed-type inhibitor, a predominantly anodic inhibitor	[43]
6	Polyaspartic acid/chitosan complex	-	-	Anodic type inhibitor	[45]
7	Polyaspartic acid + Zn ion	-	-	Mixed-type inhibitor, a predominantly anodic inhibitor	[36]
8	Cysteamine-modified polyaspartic acid	$\Delta G_{ads}^{\circ} = -34.70 \text{ kJ}\cdot\text{mol}^{-1}$ at 298 K $\Delta H_{ads}^{\circ} = -39.49 \text{ kJ}\cdot\text{mol}^{-1}$ at 298 K Physisorption and chemisorption	Langmuir adsorption isotherm	Mixed-type inhibitor, a predominantly cathodic inhibitor	[3]
9	Polyaspartic acid grafted $\beta$ -cyclodextrin	-	-	Mixed-type inhibitor, a predominantly cathodic inhibitor	[23]
10	Dopamine-modified polyaspartic acid	$\Delta G_{ads}^{\circ} = -33.15 \text{ kJ}\cdot\text{mol}^{-1}$ at 298 K Physisorption and chemisorption	Langmuir adsorption isotherm	Mixed-type inhibitor	[40]
11	Oligosuccinimide	$\Delta G_{ads}^{\circ} = -38.73 \text{ kJ}\cdot\text{mol}^{-1}$ at 298 K Physisorption and chemisorption	Langmuir adsorption isotherm	Mixed-type inhibitor, a predominantly anodic inhibitor	[29]

\* - : not mentioned

**Table 5** Biodegradation performance of modified PSI.

No	Corrosion inhibitor	Duration	Biodegradation rate	Ref.
1a	Ring-opening graft modification of polyaspartic acid	28 days	70.0%	[34]
1b	Polyaspartic acid	28 days	83.0%	
2a	Polyaspartic acid/2-amino-2-methyl-1-propanol graft copolymer	28 days	65.0%	[27]
2b	Polyaspartic acid	28 days	81.0%	
3	Chitosan-acrylic acid-polysuccinimide terpolymer	28 days	72.32%	[22]

The reactive inhibitor has low electronegativity because it tends to donate electrons rather than attract electrons.

Meanwhile, the computational study of modified PSI as a scale inhibitor was carried out on 2,2'-((2-aminoethyl)azanediyl)diacetic acid-polyaspartic acid [46]. Their calculated binding energy of 2,2'-((2-aminoethyl)azanediyl)diacetic acid-polyaspartic acid with calcium ion through a DFT method for observing the chelating ability of this scale inhibitor. The result demonstrated that modified PSI has more negative binding energy. Therefore, it has a better affinity to calcium ions.

## 9. Limitations and prospects

PSI is a precursor to other compounds. The synthesizing method of PSI must consider the number of chemicals,

energy, time, cost, and environmental safety, because further modification should be conducted. The molecular structures of PSI may need to be analyzed not only by IR spectroscopy but also using NMR spectroscopy. There has not been much research on the detailed analysis of the PSI structure, meanwhile it will provide information about the presence of irregular structures of PSI in the main chains or end groups that affect corrosion and scale inhibition efficiency. This analysis also tells us the possibility of modified PSI structures formed after further modification of PSI. In this review, modified PSI or OSI has shown good corrosion and/or scale inhibitor performance in various testing solutions, concentrations, temperatures, and pH. However, there are opportunities for observing the performance of modified PSI as a corrosion inhibitor on other metal types besides steel and other corrosive solutions. Several modified PSI, either corrosion or scale



inhibitors in Tables 1 and 2, can have double functions like other modified PSI in Table 3. Biodegradation studies of modified PSI tend to be scanty.

In contrast, the world's concern for the environment makes it essential. Hence, green corrosion and scale inhibitors need a biodegradation study as evidence of environmental safety. Furthermore, computational studies about modified PSI compounds as corrosion and/or scale inhibitors must be conducted. Computational calculations can theoretically explain the characteristics of those compounds and model molecular structure to obtain novel inhibitor compounds.

## 10. Conclusions

Global environmental pollution obligates researchers to create green corrosion and scale inhibitors. Utilization of a compound for these purposes cannot be determined by inhibition efficiency only, because the environmental impact from its applications should be taken into account. The biodegradation rate must be considered to ensure a clean and healthy environment because the use of non-biodegradable inhibitors will be limited in industrial-scale applications. The compounds can be classified as good scale and corrosion inhibitors if the corrosion/scale inhibition efficiencies are high in experimental and actual conditions. The performance of modified PSI may be developed for applications in various pH, temperatures, corrosive solutions, scale types, and exposure times. Computational calculations of quantum chemistry parameters can be used as experimental supporting data. This review presented OSI and modified PSI as scale and corrosion inhibitors. Even if some compounds do not have maximum performance yet, their inhibition efficiencies were quite good. Hence, the approaches to synthesis and modification of PSI as corrosion and scale inhibitors should continue to be developed.

The biodegradation rate can be analyzed from Biochemical Oxygen Demand (BOD) for better specific information considering BOD relations to the amount of dissolved oxygen required for decomposing organic compounds. Further study may be conducted to investigate the biodegradation activity of modified PSI. Such experimental results will be the basis for defining the corrosion and scale inhibitor safety levels.

### • Supplementary materials

No supplementary materials are available.

### • Funding

This research had no external funding.

### • Acknowledgments

None.

### • Author contributions

The Author prepared this review by himself, including the conceptualization, literature study, writing, editing, and finishing.

### • Conflict of interest


The Author declares no conflict of interest.

### • Additional information



Muhamad Jalil Baari: Researcher and Lecturer (Assistant Professor) in the Department of Chemistry, Universitas Sembilanbelas November Kolaka.

Postgraduate courses, 2016–2018 at Institut Teknologi Bandung, Department of Chemistry, Faculty of Mathematics and Natural Sciences.

Scientific interest: Physical chemistry research that focuses on material synthesis as corrosion and scale inhibitors, metal and dye adsorbent, and waste treatment. Scopus ID [57215409862](#); WOS ID AAB-7156-2021; ResearchGate .

Websites:

<http://www.usn.ac.id/>;

[https://fst.usn.ac.id/web/detail\\_dosen.php?id=42](https://fst.usn.ac.id/web/detail_dosen.php?id=42)

## References

- Mady MF, Rehman A, Kelland MA. Synthesis and study of modified polyaspartic acid coupled phosphonate and sulfonate moieties as green oilfield scale inhibitors. *Ind Eng Chem Res.* 2021;60(23):8331–8339. doi:[10.1021/acs.iecr.1c01473](#)
- Chen Y, Zhou Y, Yao Q, Nan Q, Zhang M, Sun W. Synthesis of modified polyepoxysuccinic acid and evaluation of its scale inhibition on CaCO<sub>3</sub>, CaSO<sub>4</sub>, and Ca<sub>3</sub>(PO<sub>4</sub>)<sub>2</sub> precipitation for industrial recycling water. *Desalin Water Treat.* 2019;152:16–25. doi:[10.5004/dwt.2019.23918](#)
- Chai C, Xu Y, Li D, Zhao X, Xu Y, Zhang L. Progress in organic coatings cysteamine modified polyaspartic acid as a new class of green corrosion inhibitor for mild steel in sulfuric acid medium: synthesis, electrochemical, surface study and theoretical calculation. *Prog Org Coatings.* 2019;129:159–170. doi:[10.1016/j.porgcoat.2018.12.028](#)
- Wang Q, Liang F, Al-nasser W, Al-dawood F. Laboratory study on efficiency of three calcium carbonate scale inhibitors in the presence of EOR chemicals. *Petroleum.* 2018;4:375–384. doi:[10.1016/j.petlm.2018.03.003](#)
- Rahman F. Calcium sulfate precipitation studies with scale inhibitors for reverse osmosis desalination. *Desalination.* 2013;319:79–84. doi:[10.1016/j.desal.2013.03.027](#)
- Al-Roomi YM, Hussain KF. Potential kinetic model for scaling and scale inhibition mechanism. *Desalination.* 2016;393:186–195. doi:[10.1016/j.desal.2015.07.025](#)
- Ali SA, Kazi IW, Rahman F. Synthesis and evaluation of phosphate-free antiscalants to control CaSO<sub>4</sub>·2H<sub>2</sub>O scale formation in reverse osmosis desalination plants. *Desalination.* 2015;357:36–44. doi:[10.1016/j.desal.2014.11.006](#)

8. Qiang AY, Zhang S, Yan S. Three indazole derivatives as corrosion inhibitors of copper in a neutral chloride solution. *Eval Program Plann.* 2017;126:295–304. doi:[10.1016/j.corsci.2017.07.012](https://doi.org/10.1016/j.corsci.2017.07.012)
9. Song FM, Kirk DW, Graydon JW, Cormack DE. Predicting carbon dioxide corrosion of bare steel under an aqueous boundary layer. *Corrosion.* 2004;60(8):736–748. doi:[10.5006/1.3287853](https://doi.org/10.5006/1.3287853)
10. Kumar CMP, Chandrashekarappa MPG, Kulkarni RM, Pimenov DY, Giasin K. The effect of Zn and Zn-WO<sub>3</sub> composites nano-coatings deposition on hardness and corrosion resistance in steel substrate. *Mater (Basel).* 2021;14(9):2253. doi:[10.3390/ma14092253](https://doi.org/10.3390/ma14092253)
11. Romijarso TB, Rohmah M, Tajalla GUN, Siradj ES, Mabururi E, Synergistic effect of chromium content and intercritical annealing process on corrosion-resistant improvement of Ni-Cr-Mo low alloy. *Int J Corros Scale Inhib.* 2022;11(4):1557–1568. doi:[10.17675/2305-6894-2022-11-4-8](https://doi.org/10.17675/2305-6894-2022-11-4-8)
12. Pfeifer K, Telegdi J. Improved hydrophobicity for better corrosion control by special self-assembled molecular coatings. *Int J Corros Scale Inhib.* 2022;11(3):1041–1062. doi:[10.17675/2305-6894-2022-11-3-9](https://doi.org/10.17675/2305-6894-2022-11-3-9)
13. Makarychev YB, Luchkin AY, Grafov OY, Andreev NN. Vapor-phase deposition of polymer siloxane coatings on the surface of copper and low-carbon steel. *Int J Corros Scale Inhib.* 2022;11(3):980–1000. doi:[10.17675/2305-6894-2022-11-3-6](https://doi.org/10.17675/2305-6894-2022-11-3-6)
14. Arunadevi N, Swathika M, Mehala M, Ranjith Kumar E, Bawazeer TM, Morad M, Alkhamis K, Al-nami SY, El-Metwaly NM. New epoxy-Nano metal oxide-based coatings for enhanced corrosion protection. *J Mol Struct.* 2022;1250:131790. doi:[10.1016/j.molstruc.2021.131790](https://doi.org/10.1016/j.molstruc.2021.131790)
15. Bystrov SG, Reshetnikov SM, Borisova, Pisareva, Bayankin VY. Study on the efficiency of benzotriazole and mercaptobenzothiazole as corrosion inhibitors of some high-alloy steels in neutral environment. *Int J Corros Scale Inhib.* 2022;11(2):647–658. doi:[10.17675/2305-6894-2022-11-2-13](https://doi.org/10.17675/2305-6894-2022-11-2-13)
16. Elbadaoui A, Galai M, Ferraa S, Barebita H, Cherkaoui M, Guedira T. A new family of borated glasses as a corrosion inhibitor for steel in 1.0 M hydrochloric acid: synthesis and cauterization studies. *Int J Corros Scale Inhib.* 2022;11(2):666–685. doi:[10.17675/2305-6894-2022-11-2-15](https://doi.org/10.17675/2305-6894-2022-11-2-15)
17. Bedir AG, Abd El-raouf M, Abdel-Mawgoud S, Negm NA, El Basiony NM. Corrosion inhibition of carbon steel in hydrochloric acid solution using ethoxylated nonionic surfactants based on schiff base: electrochemical and computational investigations. *ACS Omega.* 2021;6(6):4300–4312. doi:[10.1021/acsomega.0c05476](https://doi.org/10.1021/acsomega.0c05476)
18. Oh D, Zhou L, Chang D, Lee WA. Novel hydrogen peroxide stabilizer in descaling process of metal surface. *Chem Eng J.* 2018;334:1169–1175. doi:[10.1016/j.cej.2017.11.058](https://doi.org/10.1016/j.cej.2017.11.058)
19. Qu Z, Wu L, An Y, Fang R, Jin S, Yang J, Liu Y, Wang L, Yang X, Yan D. A descaling methodology for a water-filled pipe based on leaky guided ultrasonic waves cavitation. *Chem Eng Res Des.* 2019;146:470–477. doi:[10.1016/j.cherd.2019.04.027](https://doi.org/10.1016/j.cherd.2019.04.027)
20. Chen Y, Chen X, Liang Y, Gao Y. Synthesis of polyaspartic acid-oxidized starch copolymer and evaluation of its inhibition performance and dispersion capacity. *J Dispers Sci Technol.* 2021;42(13):1926–1935. doi:[10.1080/01932691.2020.1791172](https://doi.org/10.1080/01932691.2020.1791172)
21. Baari MJ, Bundjali B, Wahyuningrum D. Performance of N,O-carboxymethyl chitosan as corrosion and scale inhibitors in CO<sub>2</sub> saturated brine solution. *Indones J Chem.* 2021;21(4):954–967. doi:[10.22146/ijc.64255](https://doi.org/10.22146/ijc.64255)
22. Zheng Y, Gao Y, Li H, Yan M, Zhao J, Liu Z. Chitosan-acrylic acid-polysuccinimide terpolymer as environmentally friendly scale and corrosion inhibitor in artificial seawater. *Desalination.* 2021;520:115367. doi:[10.1016/j.desal.2021.115367](https://doi.org/10.1016/j.desal.2021.115367)
23. Fu L, Lv J, Zhou L, Li Z, Tang M, Li J. Study on corrosion and scale inhibition mechanism of polyaspartic acid grafted  $\beta$ -cyclodextrin. *Mater Lett.* 2020;264:127276. doi:[10.1016/j.matlet.2019.127276](https://doi.org/10.1016/j.matlet.2019.127276)
24. Zhang Y, Yin H, Zhang Q, Li Y, Yao P, Huo H. A novel polyaspartic acid derivative with multifunctional groups for scale inhibition application. *Environ Technol.* 2018;39(7):843–850. doi:[10.1080/09593330.2017.1312551](https://doi.org/10.1080/09593330.2017.1312551)
25. Chen Y, Xing W, Wang L, Chen L. Experimental and electrochemical research of an efficient corrosion and scale inhibitor. *Mater (Basel).* 2019;12(11):1821. doi:[10.3390/ma12111821](https://doi.org/10.3390/ma12111821)
26. Li L, Wu J, Zhao M, Wang Y, Zhang H, Zhang X, Gui L, Liu J, Mair N, Peng S. Poly- $\alpha,\beta$ -DL-aspartyl-L-cysteine: a novel nanomaterial having a porous structure, special complexation capability for Pb(II), and selectivity of removing Pb(II). *Chem Res Toxicol.* 2012;25(9):1948–1954. doi:[10.1021/tx300265c](https://doi.org/10.1021/tx300265c)
27. Shi S, Wu Y, Wang Y, Yu J, Xu Y. Synthesis and characterization of a biodegradable polyaspartic acid/2-amino-2-methyl-1-propanol graft copolymer and evaluation of its scale and corrosion inhibition performance. *RSC Adv.* 2017;7(58):36714–36721. doi:[10.1039/c7ra06848d](https://doi.org/10.1039/c7ra06848d)
28. Yu W, Wang Y, Li A, Yang H. Evaluation of the structural morphology of starch-graft-poly(acrylic acid) on its scale-inhibition efficiency. *Water Res.* 2018;141:86–95. doi:[10.1016/j.watres.2018.04.021](https://doi.org/10.1016/j.watres.2018.04.021)
29. Baari MJ, Bundjali B, Wahyuningrum D. Synthesis of oligosuccinimide and evaluation of its corrosion inhibition performance on carbon steel in CO<sub>2</sub>-saturated 1% NaCl solution. *J Math Fundam Sci.* 2020;52(2):202–221. doi:[10.5614/j.math.fund.sci.2020.52.2.5](https://doi.org/10.5614/j.math.fund.sci.2020.52.2.5)
30. Liu Z, Sun Y, Zhou X, Wu T, Tian Y, Wang Y. Synthesis and scale inhibitor performance of polyaspartic acid. *J Environ Sci.* 2011;23:S153–S155. doi:[10.1016/S1001-0742\(11\)61100-5](https://doi.org/10.1016/S1001-0742(11)61100-5)
31. Sun X, Zhang J, Yin C, Zhang J, Han J. Poly(aspartic acid)-tryptophan grafted copolymer and its scale-inhibition performance. *J Appl Polym Sci.* 2015;132(45):2–9. doi:[10.1002/app.42739](https://doi.org/10.1002/app.42739)
32. Wang X, Lv X, Zhang B, Xu B, Xu Y. Scale inhibition performance research of polyaspartic acid/diethylenetriamine graft copolymer. *J Chem Eng Japan.* 2015;48(6):506–510. doi:[10.1252/jcej.14we096](https://doi.org/10.1252/jcej.14we096)
33. Migahed MA, Rashwan SM, Kamel MM, Habib RE. Synthesis, characterization of polyaspartic acid-glycine adduct and evaluation of their performance as scale and corrosion inhibitor in desalination water plants. *J Mol Liq.* 2016;224:849–858. doi:[10.1016/j.molliq.2016.10.091](https://doi.org/10.1016/j.molliq.2016.10.091)
34. Zhou Y, Wang J, Fang Y. Green and high effective scale inhibitor based on ring-opening graft modification of polyaspartic acid. *Catal.* 2021;11(7):802. doi:[10.3390/catal11070802](https://doi.org/10.3390/catal11070802)
35. Zhang Y, Yin H, Zhang Q, Li Y, Yao P. Synthesis and characterization of novel polyaspartic acid/urea graft copolymer with acylamino group and its scale inhibition performance. *Desalination.* 2016;395:92–98. doi:[10.1016/j.desal.2016.05.020](https://doi.org/10.1016/j.desal.2016.05.020)
36. Zeino A, Abdulazeez I, Khaled M, Jawich MW, Obot IB. Mechanistic study of polyaspartic acid (PAS) as eco-friendly corrosion inhibitor on mild steel in 3% NaCl aerated solution. *J Mol Liq.* 2018;250:50–62. doi:[10.1016/j.molliq.2017.11.160](https://doi.org/10.1016/j.molliq.2017.11.160)
37. Piątkowski M, Bogdał D, Raclavský K. <sup>1</sup>H and <sup>13</sup>C NMR analysis of poly(succinimide) prepared by microwave-enhanced polycondensation of L-aspartic acid. *Int J Polym Anal Charact.* 2015;20(8):714–723. doi:[10.1080/1023666X.2016.1081134](https://doi.org/10.1080/1023666X.2016.1081134)
38. Zhang S, Qu H, Yang Z, Fu CE, Tian Z, Yang W. Scale inhibition performance and mechanism of sulfamic/amino acids modified polyaspartic acid against calcium sulfate. *Desalination.* 2017;419:152–159. doi:[10.1016/j.desal.2017.06.016](https://doi.org/10.1016/j.desal.2017.06.016)
39. Zeng D, Chen T, Zhou S. Synthesis of polyaspartic acid/chitosan graft copolymer and evaluation of its scale inhibition and corrosion inhibition performance. *Int J Electrochem Sci.* 2015;10(11):9513–9527. English. Available

- from: <http://www.electrochemsci.org/papers/vol10/101109513.pdf>. Accessed on 21 March 2022.
40. Chai C, Xu Y, Xu Y, Liu S, Zhang L. Dopamine-modified polyaspartic acid as a green corrosion inhibitor for mild steel in acid solution. *Eur Polym J.* 2020;137:109946. doi: [10.1016/j.eurpolymj.2020.109946](https://doi.org/10.1016/j.eurpolymj.2020.109946)
  41. Baari MJ, Megawati M, Benu DP. <sup>1</sup>H and <sup>13</sup>C NMR study of oligosuccinimide prepared by thermal condensation and evaluation of its scale inhibition. *JPKP.* 2022;7(3):287–302. doi: [10.20961/jpkp.v7i3.65666](https://doi.org/10.20961/jpkp.v7i3.65666)
  42. Cheng Y, Guo X, Zhao X, Wu Y, Cao Z, Cai Y, Xu Y. Nanosilica modified with polyaspartic acid as an industrial circulating water scale inhibitor. *Clean Water.* 2021;4(1):1–8. doi: [10.1038/s41545-021-00137-y](https://doi.org/10.1038/s41545-021-00137-y)
  43. Migahed MA, Rashwan SM, Kamel MM, Habib RE. Synthesized polyaspartic acid derivatives as corrosion and scale inhibitors in desalination operations. *Cogent Eng.* 2017;206(1):1–22. doi: [10.1080/23311916.2017.1366255](https://doi.org/10.1080/23311916.2017.1366255)
  44. Gao Y, Fan L, Ward L, Liu Z. Synthesis of polyaspartic acid derivative and evaluation of its corrosion and scale inhibition performance in seawater utilization. *Desalination.* 2015;365:220–226. doi: [10.1016/j.desal.2015.03.006](https://doi.org/10.1016/j.desal.2015.03.006)
  45. Chen T, Zeng D, Zhou S. Study of polyaspartic acid and chitosan complex corrosion inhibition and mechanisms. *Polish J Environ Stud.* 2018;27(4):1441–1448. doi: [10.15244/pjoes/78245](https://doi.org/10.15244/pjoes/78245)
  46. Cai YH, Zhao JL, Guo XY, Zhang XJ, Zhang RR, Ma SR, Cheng YM, Cao ZY, Xu Y. Synthesis of polyaspartic acid-capped 2-aminoethylamino acid as a green water treatment agent and study of its inhibition performance and mechanism for calcium scales. *RSC Adv.* 2022;12(38):24596–24606. doi: [10.1039/D2RA04075A](https://doi.org/10.1039/D2RA04075A)
  47. Sangeetha Y, Meenakshi S, SairamSundaram, C. Corrosion mitigation of N-(2-hydroxy-3-trimethyl ammonium)propyl chitosan chloride as inhibitor on mild steel. *Int J Biol Macromol.* 2015;72:1244–1249. doi: [10.1016/j.ijbiomac.2014.10.044](https://doi.org/10.1016/j.ijbiomac.2014.10.044)
  48. Chaudhari LP, Patel SN. Green approach to corrosion inhibition on mild steel in acidic media by the expired sulphadiazine drug. *Int J Manag Technol Eng.* 2018;8(11):665–678. English. Available from: <https://www.ijamtes.org/gallery/84.%20onov%20ijmte%20-%20oas.pdf>. Accessed on 21 March 2022.
  49. Ahamad I, Prasad R, Quraishi MA. Adsorption and inhibitive properties of some new Mannich bases of Isatin derivatives on corrosion of mild steel in acidic media. *Corros Sci.* 2010;52(4):1472–1481. doi: [10.1016/j.corsci.2010.01.015](https://doi.org/10.1016/j.corsci.2010.01.015)
  50. Barmatov E, Hughes T, Nagl M. Efficiency of film-forming corrosion inhibitors in strong hydrochloric acid under laminar and turbulent flow conditions. *Corros Sci.* 2015;92:85–94. doi: [10.1016/j.corsci.2014.11.038](https://doi.org/10.1016/j.corsci.2014.11.038)
  51. Chen J, Xu L, Han J, Su M, Wu Q. Synthesis of modified polyaspartic acid and evaluation of its scale inhibition and dispersion capacity. *Desalination.* 2015;358:42–48. doi: [10.1016/j.desal.2014.11.010](https://doi.org/10.1016/j.desal.2014.11.010)
  52. Zhang YL, Zhao CX, Liu XD, Li W, Wang, JL, Hu ZG. Application of poly(aspartic acid-citric acid) copolymer compound inhibitor as an effective and environmental agent against calcium phosphate in cooling water systems. *J Appl Res Technol.* 2016;14(6):425–433. doi: [10.1016/j.jart.2016.08.006](https://doi.org/10.1016/j.jart.2016.08.006)
  53. Yu W, Song D, Chen W, Yang H. Antiscalants in RO membrane scaling control. *Water Res.* 2020;183:115985. doi: [10.1016/j.watres.2020.115985](https://doi.org/10.1016/j.watres.2020.115985)
  54. Husna UZ, Elraies KA, Shuhili JABM, Elryes AA. A review: the utilization potency of biopolymer as eco-friendly scale inhibitors. *J Pet Explor Prod Technol.* 2022;12(4):1075–1094. doi: [10.1007/s13202-021-01370-4](https://doi.org/10.1007/s13202-021-01370-4)
  55. Huang H, Yao Q, Jiao Q, Liu B, Chen H. Polyepoxysuccinic acid with hyper-branched structure as an environmentally friendly scale inhibitor and its scale inhibition mechanism. *J Saudi Chem Soc.* 2019;23(1):61–74. doi: [10.1016/j.jscs.2018.04.003](https://doi.org/10.1016/j.jscs.2018.04.003)
  56. Oshchepkov M, Golovesov V, Ryabova A, Tkachenko S, Redchuk A, Rönkkömäki H, Rudakova G, Pervov A, Popov K. Visualization of a novel fluorescent-tagged bisphosphonate behavior during reverse osmosis desalination of water with high sulfate content. *Sep Purif Technol.* 2021;255:117382. doi: [10.1016/j.seppur.2020.117382](https://doi.org/10.1016/j.seppur.2020.117382)
  57. Ostolska I, Wiśniewska M. Comparison of the influence of polyaspartic acid and polylysine functional groups on the adsorption at the Cr<sub>2</sub>O<sub>3</sub>-Aqueous polymer solution interface. *Appl Surf Sci.* 2014;311:734–739. doi: [10.1016/j.apsusc.2014.05.149](https://doi.org/10.1016/j.apsusc.2014.05.149)
  58. Guo X, Qiu F, Dong K, Zhou X, Qi J, Zhou Y, Yang D. Preparation, characterization and scale performance of scale inhibitor copolymer modification with chitosan. *J Ind Eng Chem.* 2012;18(6):2177–2183. doi: [10.1016/j.jiec.2012.06.015](https://doi.org/10.1016/j.jiec.2012.06.015)
  59. Yang L, Li Y, Qian B, Hou B. Polyaspartic acid as a corrosion inhibitor for WE43 magnesium alloy. *J Magnes Alloy.* 2015;3(1):47–51. doi: [10.1016/j.jma.2014.12.009](https://doi.org/10.1016/j.jma.2014.12.009)
  60. Duggirala P. Formation of calcium carbonate scale and control strategies in continuous digesters. CD del II Coloq. Int. sobre Celul [internet]. 2005. English. Available from: [http://www.eucalyptus.com.br/icepo2/prasad\\_duggirala](http://www.eucalyptus.com.br/icepo2/prasad_duggirala). Accessed on 22 November 2022.
  61. Kumar S, Naiya TK, Kumar T. Developments in oil field scale handling towards green technology—a review. *J Petrol Sci Eng.* 2018;169:42–444. doi: [10.1016/j.petrol.2018.05.068](https://doi.org/10.1016/j.petrol.2018.05.068)
  62. Hajirezaie S, Wu X, Reza M, Sakha S. Numerical simulation of mineral precipitation in hydrocarbon reservoirs and wellbores. *Fuel.* 2019;238:462–472. doi: [10.1016/j.fuel.2018.10.101](https://doi.org/10.1016/j.fuel.2018.10.101)
  63. Niedermayr A, Köhler SJ, Dietzel M. Impacts of aqueous carbonate accumulation rate, magnesium and polyaspartic acid on calcium carbonate formation (6–40 °C). *Chem Geol.* 2013;340:105–120. doi: [10.1016/j.chemgeo.2012.12.014](https://doi.org/10.1016/j.chemgeo.2012.12.014)
  64. de Souza FS, Spinelli A. Caffeic acid as a green corrosion inhibitor for mild steel. *Corros Sci.* 2009;51(3):642–649. doi: [10.1016/j.corsci.2008.12.013](https://doi.org/10.1016/j.corsci.2008.12.013)
  65. Ma X, Jiang X, Xia S, Shan M, Li X, Yu L, Tang Q. New corrosion inhibitor acrylamide methyl ether for mild steel in 1M HCl. *Appl Surf Sci.* 2016;371:248–257. doi: [10.1016/j.apsusc.2016.02.212](https://doi.org/10.1016/j.apsusc.2016.02.212)
  66. Hasson D, Shemer H, Sher A. State of the art of friendly ‘green’ scale control inhibitors: A review article. *Ind Eng Chem Res.* 2011;50(12):7601–7607. doi: [10.1021/ie200370v](https://doi.org/10.1021/ie200370v)
  67. Mamand DM, Awla AH, Kak Anwer TM, Qadr HM. Quantum chemical study of heterocyclic organic compounds on the corrosion inhibition. *Chim Techno Acta.* 2022;9(2):1–11. doi: [10.15826/chimtech.2022.9.2.03](https://doi.org/10.15826/chimtech.2022.9.2.03)
  68. Baari MJ, Pratiwi RY. Application of carbon dots as corrosion inhibitor: a systematic literature review. *Indones J Chem.* 2022;22(5):1427–1453. doi: [10.22146/ijc.72327](https://doi.org/10.22146/ijc.72327)
  69. Hadisaputra S, Hamdiani S, Kurniawan MA. Influence of macrocyclic ring size on the corrosion inhibition efficiency of dibenzo crown ether : a density functional study. *Ind J Chem.* 2017;17(3):431–438. doi: [10.22146/ijc.26667](https://doi.org/10.22146/ijc.26667)
  70. Radhi AH, Du EAB, Khazaal FA, Abbas ZM, Aljelawi OH, Hamadan SD, Almashhadani HA, Kadhim MM. HOMO-LUMO energies and geometrical structures effect on corrosion inhibition for organic compounds predict by DFT and PM3 methods. *Neuro Quantal.* 2020;18(1):37–45. doi: [10.14704/nq.2020.18.1.NQ20105](https://doi.org/10.14704/nq.2020.18.1.NQ20105)
  71. Mishra A., Aslam J, Verma C, Quraishi MA, Ebenso EE. Imidazoles as highly effective heterocyclic corrosion inhibitors for metals and alloys in aqueous electrolytes: a review. *J Taiwan Inst Chem Eng.* 2020;114:341–358. doi: [10.1016/j.jtice.2020.08.034](https://doi.org/10.1016/j.jtice.2020.08.034)
  72. Ebenso EE, Isabirye DA, Eddy NO. Adsorption and quantum chemical studies on the inhibition potentials of some thiosemicarbazides for the corrosion of mild steel in acidic

- medium. *Int J Mol Sci.* 2010;11(6):2473–2498. doi:[10.3390/ijms11062473](https://doi.org/10.3390/ijms11062473)
73. Fujimoto H, Inagaki S. Orbital interaction and chemical bonds. Polarization in chemical reactions. *J Am Chem Soc.* 1977; 99(23):7424–7432. doi:[10.1021/ja00465a004](https://doi.org/10.1021/ja00465a004)

## 10 Most important cited papers

1. Baari MJ, Bundjali B, Wahyuningrum D. Synthesis of oligosuccinimide and evaluation of its corrosion inhibition performance on carbon steel in CO<sub>2</sub>-saturated 1% NaCl solution. *J Math Fundam Sci.* 2020;52(2):202–221. doi:[10.5614/j.math.fund.sci.2020.52.2.5](https://doi.org/10.5614/j.math.fund.sci.2020.52.2.5)
2. Liu Z, Sun Y, Zhou X, Wu T, Tian Y, Wang Y. Synthesis and scale inhibitor performance of polyaspartic acid. *J Environ Sci.* 2011;23:S153–S155. doi:[10.1016/S1001-0742\(11\)61100-5](https://doi.org/10.1016/S1001-0742(11)61100-5)
3. Qiang AY, Zhang S, Yan S. Three indazole derivatives as corrosion inhibitors of copper in a neutral chloride solution. *Eval Program Plann.* 2017;126:295–304. doi:[10.1016/j.corsci.2017.07.012](https://doi.org/10.1016/j.corsci.2017.07.012)
4. Zeng D, Chen T, Zhou S. Synthesis of polyaspartic acid/chitosan graft copolymer and evaluation of its scale inhibition and corrosion inhibition performance. *Int J Electrochem Sci.* 2015;10(11):9513–9527. Available from:<http://www.electrochemsci.org/papers/vol10/101109513.pdf>. Accessed on 21 March 2022.
5. Biswas A, Pa S, Udayabhanu G. Experimental and theoretical studies of xanthan gum and its graft co-polymer as corrosion inhibitor for mild steel in 15% HCl. *Appl Surf Sci.* 2015;353:173–183. doi:[10.1016/j.apsusc.2015.06.128](https://doi.org/10.1016/j.apsusc.2015.06.128)
6. Baari MJ, Bundjali B, Wahyuningrum D. Performance of *N,O*-carboxymethyl chitosan as corrosion and scale inhibitors in CO<sub>2</sub> saturated brine solution. *Indones J Chem.* 2021;21(4):954–967. doi:[10.22146/ijc.64255](https://doi.org/10.22146/ijc.64255)
7. Zhou Y, Wang J, Fang Y. Green and high effective scale inhibitor based on ring-opening graft modification of polyaspartic acid. *Catalysts.* 2021;11(7):802. doi:[10.3390/catal11070802](https://doi.org/10.3390/catal11070802)
8. Kamal MS, Hussein I, Mahmoud M, Sultan AS, and Saad MAS. Oilfield scale formation and chemical removal: A review. *J Pet Sci Eng.* 2018;171:127–139. doi:[10.1016/j.petrol.2018.07.037](https://doi.org/10.1016/j.petrol.2018.07.037)
9. Piątkowski M, Bogdał D, Raclavský K. <sup>1</sup>H and <sup>13</sup>C NMR analysis of poly(succinimide) prepared by microwave-enhanced polycondensation of L-aspartic acid. *Int J Polym Anal Charact.* 2015;20(8):714–723. doi:[10.1080/1023666X.2016.1081134](https://doi.org/10.1080/1023666X.2016.1081134)
10. Singh P, Chauhan DS, Srivastava K, Srivastava V, Quraishi MA. Expired atorvastatin drug as corrosion inhibitor for mild steel in hydrochloric acid solution. *Int J Ind Chem.* 2017;8(4):363–372. doi:[10.1007/s40090-017-0120-5](https://doi.org/10.1007/s40090-017-0120-5)